Geothermal Deep Direct Use for Turbine Inlet Cooling in East Texas

Craig Turchi,[1][*] Josh McTigue,[1] Sertaç Akar,[1] Koenraad Beckers,[1] Maria Richards,[2] Cathy Chickering,[2] Joseph Batir,[2] Harrison Schumann,[2] Tom Tillman,[3] and David Slivensky[4]

[1] *National Renewable Energy Laboratory*
[2] *Southern Methodist University*
[3] *TAS Energy*
[4] *Eastman Chemical Company*

[*] *Project PI*

Geothermal Deep Direct Use for Turbine Inlet Cooling in East Texas

Craig Turchi,[1*] Josh McTigue,[1] Sertaç Akar,[1] Koenraad Beckers,[1]
Maria Richards,[2] Cathy Chickering,[2] Joseph Batir,[2]
Harrison Schumann,[2] Tom Tillman,[3] and David Slivensky[4]

[1] *National Renewable Energy Laboratory*
[2] *Southern Methodist University*
[3] *TAS Energy*
[4] *Eastman Chemical Company*

[*] *Project PI*

Foreword

The National Renewable Energy Laboratory (NREL), the Southern Methodist University Geothermal Laboratory (SMU), Eastman Chemical, and TAS Energy (Houston, TX) evaluated the deep direct-use application of geothermal energy to improve the efficiency of a natural gas power plant through the application of turbine inlet cooling. The primary focus area is a 10-km radius from the Eastman Chemical plant in Longview, Texas near the intersection of Gregg, Rusk, Harrison, and Panola counties. The site was selected based on the geothermal resource related to the relatively high heat flow of the geological Sabine Uplift region, as well as Eastman Chemical's proactive interest in renewable energy technologies and energy efficiency.

Acknowledgments

List of Acronyms

BHT	Bottom Hole Temperature
BSL	Base Sea Level
CV	Coefficient of Variation
DDU	Deep Direct Use
EGS	Enhanced Geothermal Systems
GEOPHIRES	Geothermal Energy Production of Heat Electricity Economically Simulated
GT	Gas Turbine
HR	Heat Rate
HRSG	Heat Recovery Steam Generators
LCOH	Levelized Cost of Heat
LPM	Lumped Parameter Model
NGDS	National Geothermal Data System
NPV	Net Present Value
NREL	National Renewable Energy Laboratory
PNNL	Pacific Northwest National Laboratory
RFC	Reservoir Flow Capacity
RPI	Reservoir Productivity Index
SAM	System Advisor Model
SMU	Southern Methodist University
TaD	Temperature at Depth
TAS	TAS Energy formerly known as Turbine Air Systems
TIC	Turbine Inlet Cooling

Executive Summary

The National Renewable Energy Laboratory (NREL), the Southern Methodist University Geothermal Laboratory (SMU), Eastman Chemical (Longview, TX), and TAS (Houston, TX) evaluated the feasibility of using geothermal heat to improve the performance of a natural-gas power plant in East Texas. The area of interest is the Eastman Chemical plant in Longview, Texas, which is on the northwestern margin of a geologic region known as the Sabine Uplift. The feasibility study focused on determining the potential for accessing a subsurface hydrothermal resource within a 10-km radius of the site to provide thermal energy for absorption chillers. Wells within a 20-km radius are included for broader geological comparison to determine the heat flow, temperature-at-depth, field porosity and permeability. The lithologies of most interest are the Lower Cretaceous Trinity Group and Upper Jurassic Cotton Valley Group. The deeper Cotton Valley formations are hotter (averaging 117 to 130°C), yet permeability and porosity are low. The shallower Trinity Group formations contain more variability in permeability and porosity and lower temperatures averaging about 98 to 117°C. These shallower formations are considered despite the lower temperature because of increased ability to produce larger volumes of water and extract enough heat before reinjection. The complete SMU analysis of reservoir potential is available in the National Geothermal Data System (NGDS).

Tapping such deep geothermal sources for direct heating (as opposed to power generation) is known as geothermal deep direct use (DDU). Geothermal DDU has potential across a wide swath of the United States but is underutilized due to challenging project economics associated with developing a deep geothermal resource for what are typically small-scale, variable-demand projects. This project examines the feasibility of geothermal energy integration in a natural-gas combined cycle power station in East Texas. The DDU resource is tapped to drive absorption chillers (24/7) for production of chilled water at 5-10°C (41-50°F). This chilled water is stored until needed, which allows for continuous operation with a relatively small-capacity geothermal/absorption chiller system. When conditions are favorable, the chilled water is dispatched to cool the air entering the compressor stage of a gas combustion turbine. This process, known as turbine inlet cooling (TIC), boosts power production during periods of high ambient temperature and high power demand. Such systems can enhance grid reliability and reduce the cost for peak-demand power.

A simulation model of the power plant was developed in IPSEpro software and validated against operational data from the plant. This model allowed the team to estimate the additional power that could be produced by applying TIC under different operating and ambient conditions. Absorption chiller performance was estimated from vendor sources to determine the production rate of chilled water from the geothermal resource. Geothermal drilling and development costs were estimated using NREL's GEOPHIRES 2.0. The expected lower drilling costs in this region, consistent with "Int1" drilling costs from (Lowry et al. 2017), set a well cost of about $3 million and led to an estimated cost of geothermal heat of about $4/MMBtu (1.4 cents/kWh$_t$). The estimated cost for the absorption chillers and TIC hardware were obtained from literature sources and project partners.

Hourly data were obtained for weather, natural gas and electricity prices, and plant operating state for 2017, which served as a representative year. NREL estimated the capital cost, operating cost, and additional electricity production and revenue for different combinations of geothermal

capacity, chiller capacity, and water storage-tank size. The analysis drove toward smaller geothermal and chiller systems to reduce equipment cost. A relatively low-cost water storage tank accumulated the near-continuous chilled water output for later use when TIC was most valued.

Project economics were explored by calculating a simple payback period and a Net Present Value (NPV), the latter using financial assumptions taken from NREL's System Advisor Model (SAM). The shortest payback period for a plant mimicking operations of the Eastman Chemical plant and using the baseline geothermal assumptions was about 45 years. Lower cost geothermal energy and greater operating capacity factor (i.e., more typical of a merchant power plant) led to payback periods as short as 10 years and positive NPV scenarios. Project life was assumed to be 30 years for the NPV calculations. Such a time frame is more aligned with utility projects than industrial plant investments. The economics were most sensitive to dispatch logic for the TIC system and whether a reduction in heat rate (i.e., increase in thermal efficiency) is obtained during TIC. TIC systems normally result in an improvement in heat rate, but this must be calculated throughout the year, for example on an hourly basis, to quantify the overall net benefit. The current study bounded the likely improvement in heat rate as between 1% and 2%. In addition to heat rate effects, it was essential for TIC system dispatch to track with electric power market prices to maximize revenue.

The estimated cost for geothermal heat in the subject location was relatively low, due to lower drilling costs in this region, which has extensive oil & gas exploration and different subsurface conditions than traditional geothermal sites. However, the study did not lead to economic deployment options for TIC in this location, because the economics were not governed by the geothermal energy costs. Conditions leading to better economics include locations with wider electric price fluctuations, greater TIC capacity factor, and the ability to realize increased power cycle efficiency in addition to increased power when applying TIC.

Table of Contents

List of Figures

List of Tables

1 Background

Geothermal energy remains an underutilized resource in the United States, with the only substantial deployment occurring in western states such as California and Nevada that have conventional high-temperature hydrothermal assets. Deployment beyond these areas will require use of unconventional technology such as enhanced geothermal systems (EGS) or greater use of low-temperature resources. The latter have found use in scattered, small-capacity systems for greenhouse heating, aquaculture, pools and spas, and district heating (Figure 1). While such beneficial use can be cost effective, the applications tend to be small and subject to "one-off" characteristics that are not conducive to regional or national deployment.
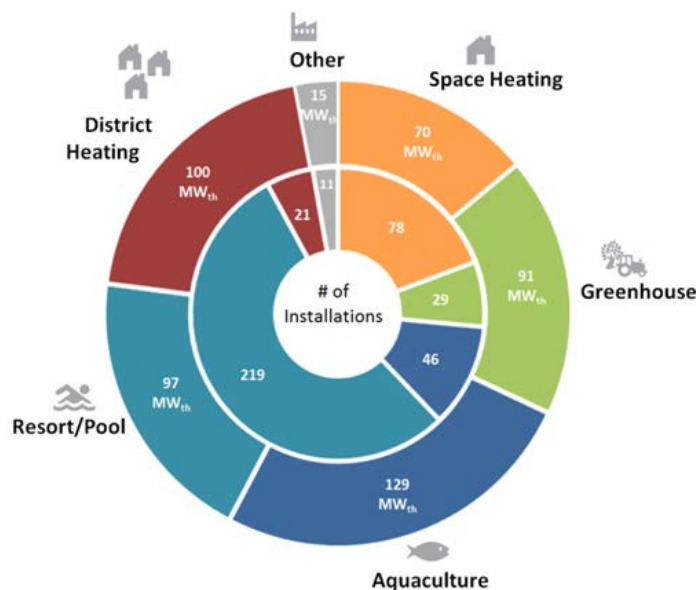
Figure 1. Current geothermal direct-use applications in the United States (Snyder, Beckers, and Young 2017).

When compared to these traditional direct-use applications, the possible integration of geothermal heat into thermo-electric power plants represents a large-scale opportunity with nationwide potential. For example, one of the largest current direct-use applications is district heating systems that total 21 systems with an average capacity of about 5 MW_t (Snyder, Beckers, and Young 2017). A single turbine inlet cooling application for an average-size 500 MW_e combined cycle power station could be as large as 54 MW_t, 11-fold larger than the average district-heating system and of a scale similar to the combined installed capacity of all geothermal district heating facilities in the United States (EPRI 2002). With approximately 2200 thermo-electric power plants in the United States, the possibilities for significant geothermal augmentation are good, should suitable subsurface resources be nearby. Regions of Texas represent a compelling case for exploring power-plant augmentation with geothermal energy.

This research documents the thermo-electric power plants and proximate geothermal resource of East Texas and determines the technical and economic potential of applying those resources to augment the output of the plants with renewable geothermal energy. The project includes participation and cost share commitment from two industry partners: Eastman Chemical,

owner/operator of a combined-cycle cogeneration plant near Longview, TX, and Houston-based TAS (formerly known as Turbine Air Systems) a provider of industrial turbine inlet cooling (TIC) systems.

Turbine inlet cooling via mechanical or absorption chillers is an established method that can improve the efficiency and reduce air emissions of gas-combustion turbines and combined-cycle power stations. Various forms of turbine inlet cooling are employed in hot climates to boost gas turbine output. However, as normally employed, these techniques all draw parasitic heat and/or power from the host plant to perform the intended operation, thereby reducing the net benefit. This project assesses the feasibility of geothermal energy integration in a natural-gas combined cycle power station in the Sabine Uplift region of East Texas to quantify the economic potential of using a low-temperature geothermal resource for TIC. The feasibility study evaluates the local geothermal resource, models integration options, and assesses economic viability.

The project originally proposed to also include the study of geothermal-heated coal drying at a coal-fired power plant in the region. Fuel drying can improve efficiency and reduce emissions at coal-fired boilers (Bullinger 2010). However, this task was dropped due to funding constraints and lack of a commercial host site. While such an application may have exhibited favorable economics for a baseload coal plant, such plants are becoming scarcer in the U.S. electric grid.

As requested by DOE, the Final Report summarizes project objectives and milestones in Table 1. SMU led the Resource Characterization task while NREL led Tasks 2 and 3 addressing system modeling and techno-economic assessment. Project partners Eastman Chemical and TAS provided essential input and review.

Table 1. Project milestones list and location within this report.

Task Name	Milestone Number	Milestone Description	Report page or location
Task 1.0 Resource Characterization	M1.1	Initial assessment of geothermal resource and plant suitability	15-18
	M1.2	Database of well and other subsurface data with 10-km radius of site	NGDS
	M1.5	Tabulated Reservoir Productivity Index (RPI) results uploaded to NGDS	NGDS
	M1.6	Permitting assessment	Appendix 2
Task 2.0 Geothermal Integration Modeling: Turbine Inlet Cooling	M2.1	Natural-gas combined cycle plant simulation model matches heat rate prediction within 5% for the same plant design	23-24
	M2.2	Process schematic and analysis of the TIC process	Appendix 1
	M2.3	Integrated performance results: Relative comparison of case study site with and without TIC indicating >10% increase in power output during hot, humid afternoons (90°F and 60%RH).	Figure 20

2

Task Name	Milestone Number	Milestone Description	Report page or location
Task 3.0 Techno-economic Assessment	M3.1	Geothermal resource cost model: Table of delivered geothermal energy (MW_t with brine temperature and mass flow rate) as a function of well depth, RPI, drilling and completion costs, and brine transport costs.	17ff
	M3.2	Net Present Value estimates for case study sites: Documentation to include process schematics and major component specifications, climate and financial assumptions, including revenue from generated electricity.	26ff
	M3.3	Stakeholder workshop	-

1.1 Prior Geothermal Integration Studies

NREL previously analyzed the use of low-temperature geothermal energy to provide feedwater heating for a steam-Rankine concentrating solar power plant (Turchi et al. 2014). The analysis indicated significant benefits: power output could be increased by 8% for the same solar-thermal input with a 150°C geothermal resource while the efficiency of converting that geothermal energy into electricity was twice that of a conventional geothermal power plant that used the same resource.

In studies involving coal-fired Rankine cycles, (Bruhn 2002) analyzed geothermal feedwater heating for power stations in Germany. The study explored the influence of drilling depth, resource temperature, and distance from geothermal wells to coal plant. Bruhn predicted that cost-effective hybrids could be developed to utilize existing technology, with well cost and brine-transport distance as key parameters. Similarly, (Zhou, Doroodchi, and Moghtaderi 2014) studied geothermal-assisted coal-fired power systems in Australia. They found that the hybrids utilizing a 120°C to 150°C resource and operating in "booster mode" produced 3-5% more power than the fossil-fuel-only plant. Operating in a "fuel saving mode," with the same resource reduced the fuel consumption by 3-4%. Thus, there is potential to increase power output or decrease fuel use.

Pacific Northwest National Laboratory (PNNL) looked at coal-fired power augmented by geothermal brines for feedwater heating or heating CO_2 capture processes (Bearden et al. 2016). PNNL noted that Louisiana/East Texas held at least three coal plants with favorable characteristics for such integration but chose to study other locations.

Most prior studies examined feedwater heating due to its known technical benefits; however feedwater-heating with geothermal energy has several limitations: (1) modern steam plants do not run constantly and geothermal resources need to be utilized continuously and at constant capacity for best economics, (2) a retrofit feedwater-heating integration is intrusive and may require major modifications to the hardware or operations of the existing power station, and (3) the U.S. generation fleet is dominated by natural-gas combined cycle plants that do not benefit from this type of integration. The integration approach in this research aims to avoid these limitations by focusing on TIC at natural-gas combined cycle power stations.

3

This approach allows one to design a smaller-capacity geothermal system that will operate 24/7 and stockpile a valued resource–chilled water–that can be used at a rate that differs from that of the geothermal system. Secondly, the geothermal system operates independently from the thermo-electric power system and interfaces with that process by chilled inlet air at a rate that can be varied to align with the needs of the power plant. As such, a retrofit application requires relatively little change to the existing plant.

1.2 Low-Temperature Geothermal Resource in Texas

The greatest technical risk in the proposed work was insufficient geothermal resource in close proximity to the plant sites. The study region has been chosen to align with known areas of low-temperature resource in East Texas and Western Louisiana. SMU's team leveraged the extensive well database for the region to examine the resource potential in a 10-km radius of the power plant site to vet the quality and depth of the geothermal resource.

SMU's "I-35 Corridor East" geothermal assessment completed in 2010 for the Texas State Energy Conservation Office (Blackwell, Richards, and Stepp 2010) highlights an area of high heat flow along the Sabine Uplift in East Texas. The I-35 Corridor East project focused on temperature mapping of thousands of wells with depths of at least 7,000 feet in the eastern half of the Texas between interstate I-35 and the Texas-Louisiana border and encompassed North, East, and South Texas, including the large population centers along the Texas Gulf Coast. Temperature-at-depth maps at multiple depth intervals were created that will provide the basis for this deep direct-use (DDU) project analysis. The large region exhibits good potential for low-temperature direct-use applications with the power plants in the region (Figure 2).
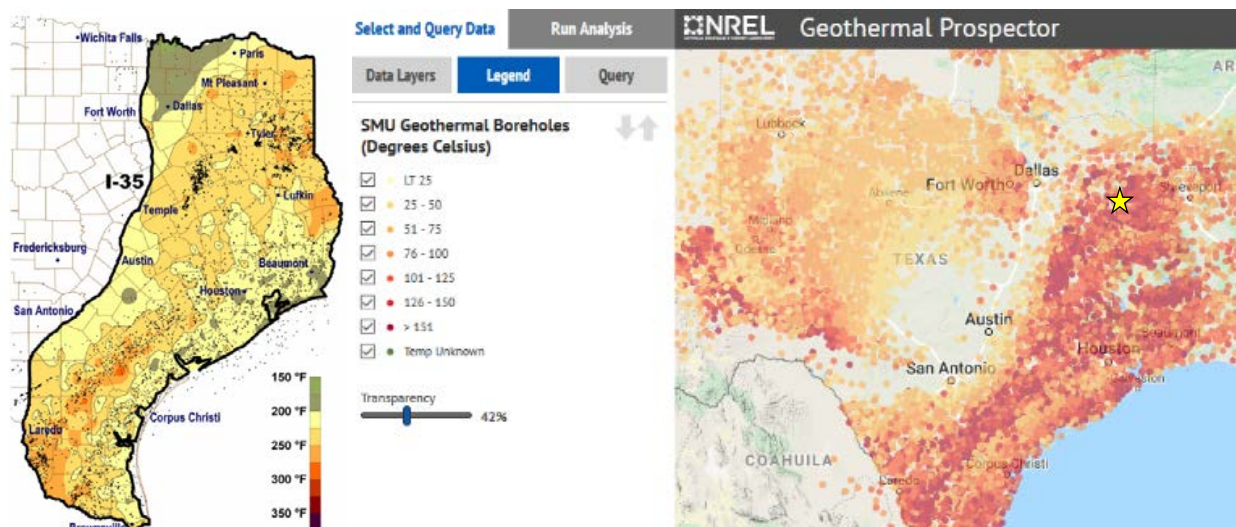
Figure 2. Proposed study area shows Texas geothermal resources at 9,000 ft depth (left). Well bottom-hole temperatures from the SMU-NGDS database are shown at right. The yellow star locates project partner Eastman Chemical's plant near Longview, TX, https://maps.nrel.gov/

1.2.1 Regional Geology

East Texas and Western Louisiana are active oil and gas plays that include the East Texas oil field, the broader East Texas Basin including the current Haynesville Shale play, and the Sabine

4

Uplift. The oil formations are shallow (Woodbine), the deeper gas formations are tight with narrow lenses of production (Dyman and Condon 2006; Ambrose et al. 2009; Dutton et al. 1991). This geological region today is north of the Gulf Coastal plains, yet during the depositional timeframe of Middle Jurassic to the Middle Cretaceous the region varied between shallow marine to shoreline depositional environments (Hammes, Hamlin, and Ewing 2011; Thomas E. Ewing 2001). A recent core review (Ambrose, Dutton, and Loucks 2017) of the Cotton Valley to the northeast of our area of interest in Harrison County, highlights the site-specific lenses of sands from very fine to medium sandstone to mudstones as the site moves through the shallow marine shelf, shoreface, tidal channel, to transgressional deposits similar to the Gulf Coastal depositional settings of today. Two salt pillows, one on the west side of the 10-km radius region of interest and another directly north along the 20-km radius are an extension of the deeper Louann Salt just above the basement rocks (Figure 3).
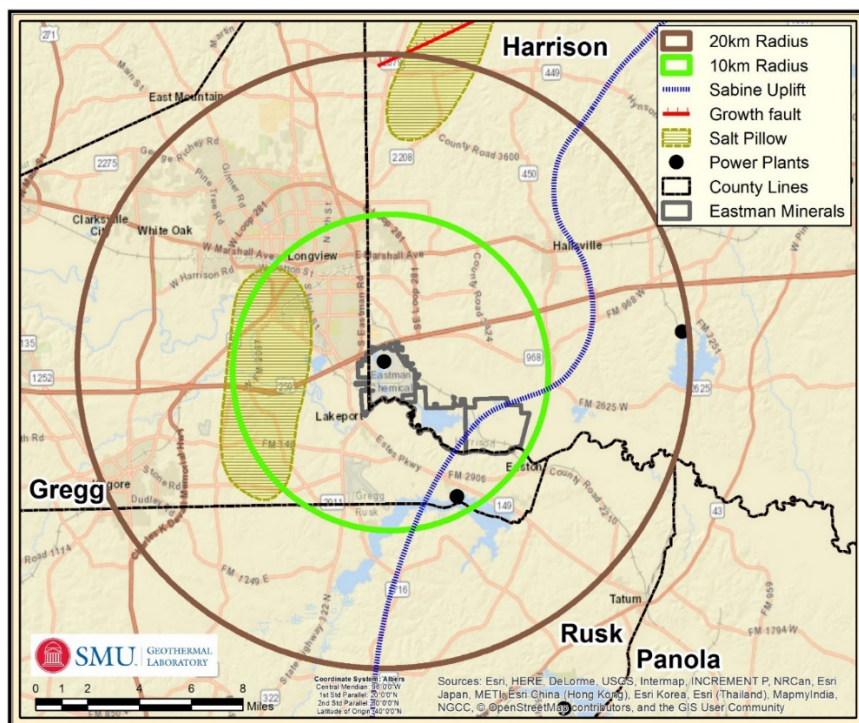
Figure 3. Map of Feasibility Area showing relevant geologic features. Eastman-owned mineral rights lie along the boundary of the Sabine Uplift (blue dashed line). The only known fault is directly north (red line). Salt pillows are located to the west and north, yet too deep to impact the local thermal regime. Counties in the area are demarked by black borders: Gregg, Harrison, Panola, and Rusk.

Referring to Figure 4, the lithologies of interest in this feasibility study are the Lower Cretaceous Trinity Group (Travis Peak / Hosston, James, Pettet / Sligo) at depths between approximately 1700 m to 2500 m and the Upper Jurassic Cotton Valley Group (Schuler and Bossier) (approximately 2500 m to 3350 m). Below these are the Haynesville and/or Smackover formations expected to be 150°C+ at approximately 3.5 km. If drilling costs are reduced these lower formations could be considered for future geothermal exploration opportunities for both DDU and electrical production.

5
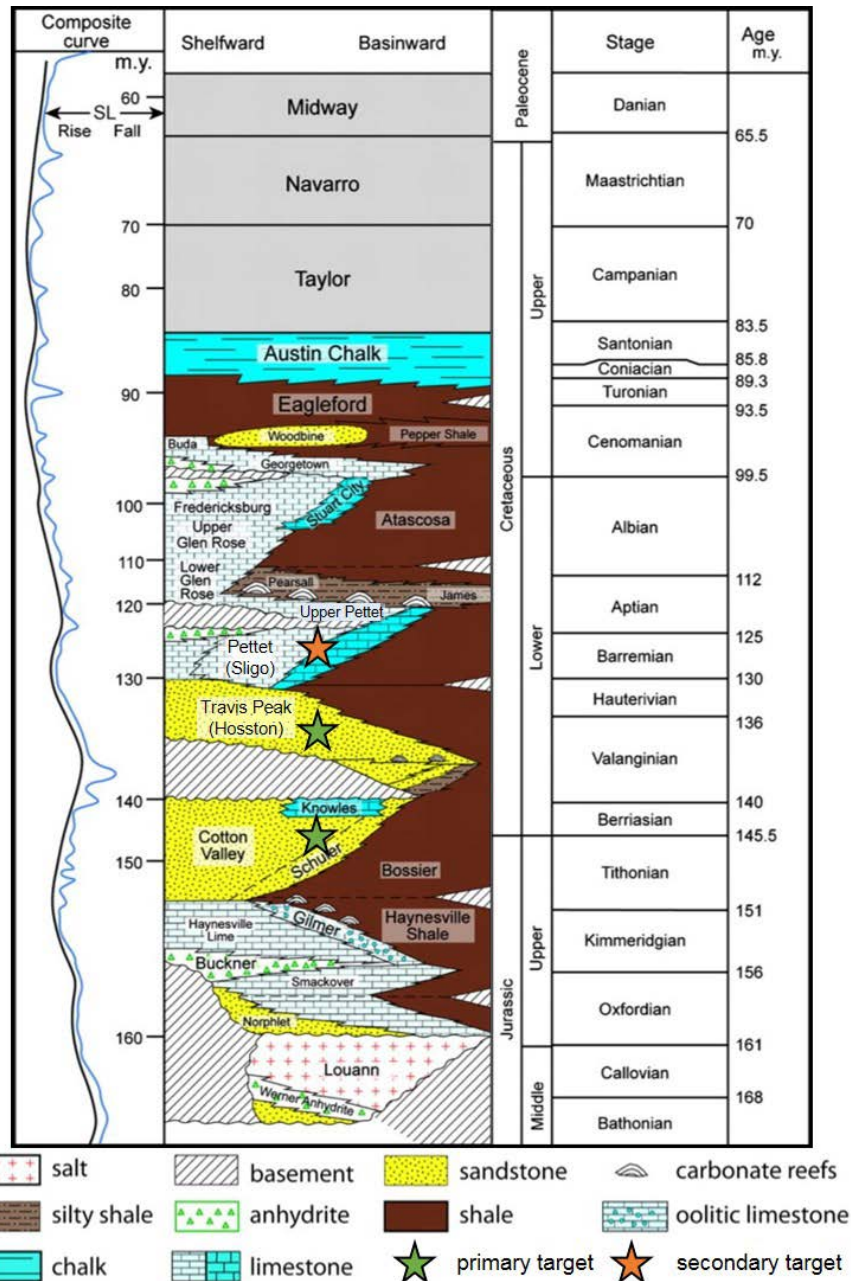
Figure 4. Generalized lithology-stratigraphic section for East Texas (modified after (Hammes, Hamlin, and Ewing 2011). The section shows how the rock type varies spatially for a given time period depending on proximity to the shelf (near shore shallow water) or basin (offshore deeper water). Target formations are marked by stars within the Upper Jurassic and Lower Cretaceous.

1.2.2 Heat Flow, Temperature-at-Depth, Heat-in-Place

The surface heat flow calculations follow the previous work by Blackwell et al. 2011 for the U.S. and the updated codes written by Cornell (Smith 2016; Smith and Horowitz 2016). Well-site-specific temperatures generate the thermal gradient by subtracting the surface groundwater temperature (Gass 1982) from the site well-log header's bottom-logged depth temperature (aka Bottom Hole Temperature, BHT). The thermal conductivity model incorporates published

6

formation estimates for the Gulf Coast (Pitman and Rowan 2012), and for the deeper Louann salt formation, the Anadarko Basin evaporite value was used (Gallardo and Blackwell 1999). The thermal conductivity for each well is given a weighted-average value to use in the heat flow calculation, i.e., thermal conductivity times gradient. From the site-by-site surface heat flow values, the dataset is gridded to depict a regional heat flow map (Figure 5). For additional understanding of parameters and calculations consult the NGDS ("NGDS" 2019).

The regional heat flow for this 20-km radius area varies from 65 to 95 mW/m^2. These values are on average about 5 to 10 mW/m^2 higher than the previously calculated heat flows for the 2011 Geothermal Map of United States (Blackwell et al. 2011). The primary reason for the increase is the thermal conductivity values used are specific to the formations within the Gulf Coast (Pitman and Rowan 2012) unlike the U.S. map that used similar thermal conductivity values for all basins related to the average of their rock types or a generalized model related to age (Blackwell et al. 2011). There is some variability in the heat flow, although similar to the gradient, the values tend to be highest in the eastern half. A heat flow of 55 to 65 mW/m^2 is considered normal for the Great Plains, therefore there is more stored thermal energy in the Longview area than in many portions of the Central United States. This increase in heat is related to the basement rock below the Sabine Uplift.
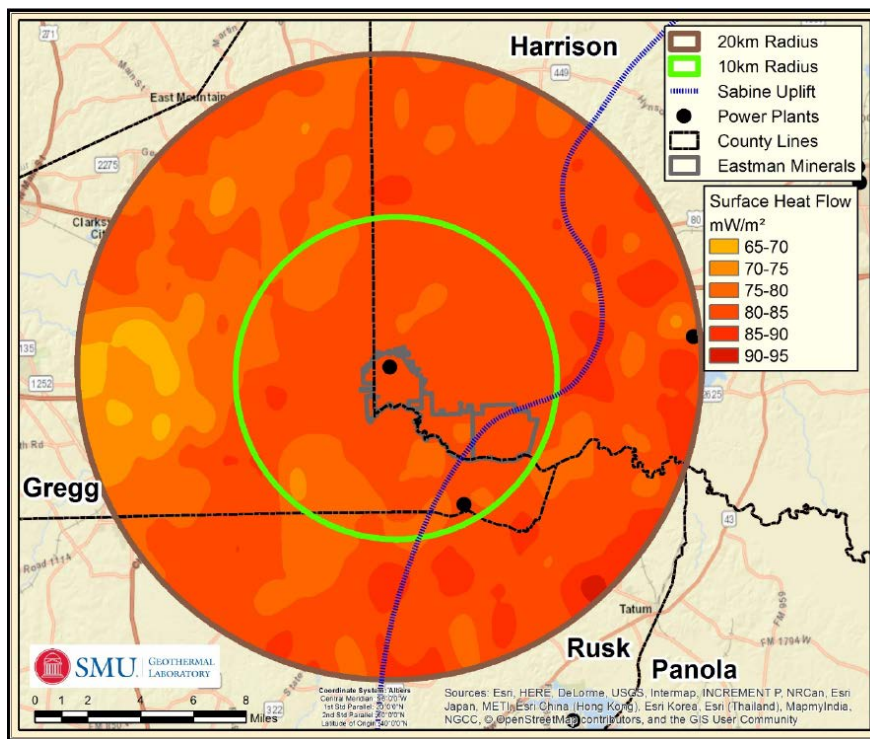
Figure 5. Surface Heat Flow of the Feasibility Study Area. The surface heat flow contour is 5 mW/m^2 with a general trend of higher heat flow to the East.

The Temperature-at-Depth (TaD) calculations are an add-on to the heat flow calculations. Temperatures are more useful in a project such as this one than heat flow. Therefore we calculated the depth to a specific temperature, and the temperature at a specific depth. Using these calculations for total heat capacity of a volume (height times area times temperature), or drilling expenses (drill cost per meter times depth to a specific temperature isotherm) are two possible applications of the temperature-depth calculations (Stutz et al. 2012). The Stutz et al. (2012) code is designed to determine temperatures to the basement formation and incorporates

7

surface heat flow, radiogenic heat production, sediment thickness, and known BHT. The results of these calculations are used for the inputs in the GEOPHIRES model and others related to reservoir potential. For additional understanding of parameters and calculations see ("NGDS" 2019).

Heat-in-Place calculations follow the Zafar and Cutright (2014) use of ArcGIS raster data previously generated in the Heat Flow and TaD calculations. The Heat-in-Place outputs provide the total thermal energy stored within a defined 3D volume. This is not the total amount possible to extract, as that changes with new technology or the life span of a project. These calculations are instead based on cell size, it can then be changed to examine different reservoir sizes based on project consumption, surface mineral right leases, or direct-use application requirements.

In reviewing the heat flow, TaD, and heat-in-place values we took into consideration the two large salt pillows shown on the Tectonic Map of Texas (Ewing 1991). Although these are both outside the primary area of interest (the closest one is west of Longview city limits), we reviewed their potential for a thermal impact in our overall calculations. Two factors were reviewed with respect to the vicinity over the salt pillows: 1) a change in elevation (BSL) of formation tops, and 2) change in trend of temperatures in the area. Neither of these factors show any direct impact of a large salt body. Therefore, it was determined that these are too deep (below the Haynesville, Figure 4) and too small to impact this study. If the results were applied to the other power plants in the broader area being mapped, these are even further from the mapped salt pillows than the Eastman Chemical mineral land area.

As part of the feasibility study there are different models for determining the potential for stored thermal energy at different reservoir depths. An example of the heat-in-place estimation technique most recently updated by Zafar and Cutright (2014) is shown here as a heat density map in Figure 6. For this map the difference between the Travis Peak Top and Cotton Valley Top (i.e., Travis Peak formation thickness) is used as the third dimension for volume (m^3) to provide heat (joules) for this density calculation (MJ/m^3). Higher values (yellows or 275-300 MJ/m^3) are primarily from higher gradients or thickness increases. There are a few higher heat density areas of interest adjacent to the Eastman Chemical property. Locations such as these can be looked into further with the details of the well logs along the cross-sections.
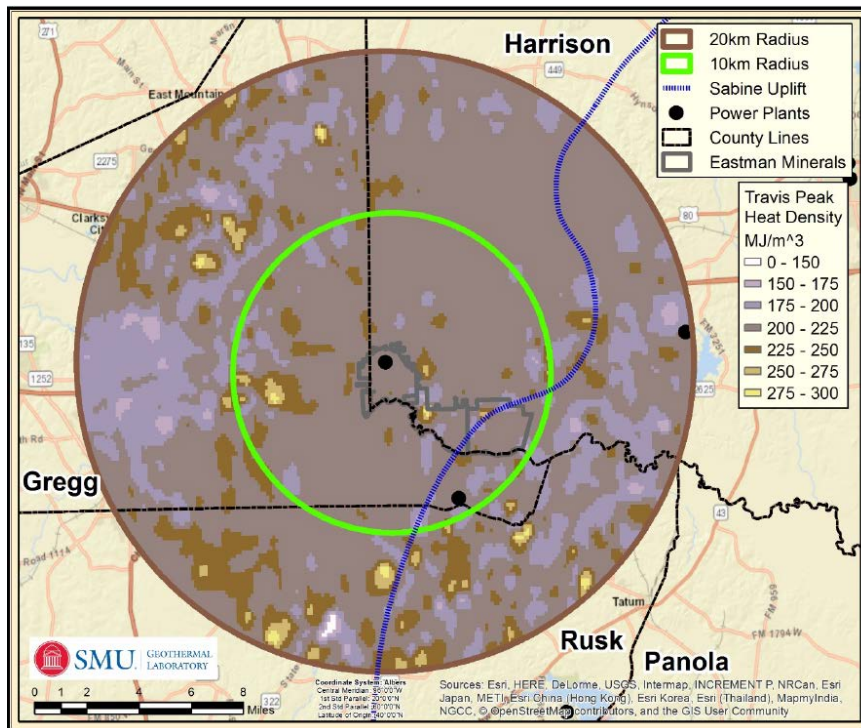
Figure 6. Travis Peak Heat Density Map based on the model of Zafar and Cutright (2014). This map represents the amount of heat contained in a slice of Earth, e.g., Travis Peak formation. The center of the map, where the Eastman Chemical mineral rights are located (dark grey outline), is within a zone of 200 to 225 MJ/m³. Map also shows the potential for variability even at formation scale.

1.2.3 Geothermal Reservoir Capacity

There are three reservoir models (Reservoir Productivity Index, Reservoir Flow Capacity, and Lumped Parameter Model) used to determine and compare the results for the potential reservoir characteristics. A detailed explanation of the codes, parameters, and files used for a step-by-step process of how the results were accomplished has been uploaded to the NGDS ("NGDS" 2019). Each method is briefly described below.

Reservoir Productivity Index and Reservoir Flow Capacity

For the Reservoir Flow Capacity (RFC) and Reservoir Productivity Index (RPI) models we collected raw data from oil and gas producing zones within regional fields to gain the extremes of temperature and formation parameters (most commonly available are thickness, porosity, permeability, and water saturation). The producing zone for the oil and gas industry is usually only the upper portion of the liquids in the formation; therefore, to improve on the possible reservoir thickness, we reviewed the injection data for length of casing perforations for a different thickness constraint within the formations. The maximum thickness possible for each formation is the average of the total thickness across the area of interest.

These reservoir parameters are used to calculate the RFC. The RFC is based on the permeability (k) in mD times reservoir thickness (H) in meters of each formation within a field and is a simple comparison of potential total fluid flow. (Camp et al. 2018) assigned reservoirs as favorable with RFC of $\geq$ 1000 mD-m.

The RPI calculation is designed to look at the productivity based on additional input parameters for a field. Values less than an RPI of 10 kg/MPa-s represent reservoirs needing stimulation. The higher the RPI the more likely a well is to be productive in a specific field or formation.

9

A series of Monte Carlo calculations incorporate the above data using a code initially developed by (Camp et al. 2018) and outputs both RPI and RFC. The updated code now inputs from and outputs to related NGDS Content Models (data input–Hydraulic Properties Observations, data output–Geologic Reservoir). The code also outputs the RFC for each geologic unit at defined locations (fields). The Monte Carlo simulation of RPI and RFC provides the 10th, 25th, 50th, 75th, and 90th percentiles along with their Coefficient of Variation (CV) to analyze the probability of the reservoir characteristics. The lower the CV the smaller the standard deviation relative to the mean, and hence the more confident are the RFC and RPI values.

The RPI formula is shown below (Equation 1) with permeability (k) in meters squared, formation/field thickness (H) in meters, viscosity (μ) in pascals per second, D the distance between the injection and production wells in meters, and the wellbore radius (r_w) in meters.

$$RPI = \frac{2\pi kH}{\mu \ln\frac{D}{r_w}} \tag{1}$$

A few assumptions were made for variables in the RPI formula. Since the wellbore radius and the distance between the injection and production wells are not known values, the values for D was set equal to 1000 m and r_w was set to 0.1 m, following values used by Camp (2016). Water viscosity is a function of temperature and pressure, which vary depending on the specific modeled formation. For simplicity, we used Camp`s (2016) value of $\mu = 0.000299$ Pa-s for water at temperatures greater than 90°C because that is the minimum temperature being examined within this study. Most of the data sources did not specify if the recorded permeability values were the permeability of gas or water; therefore, no correction was made to these values. To create random values for the simulation that reflect the variables' most likely occurrence, a log-normal distribution was used for permeability and a triangular distribution for thickness.

Lumped Parameter Model

The Lumped Parameter Model (LPM) uses reservoir parameters for total reservoir potential and computations for the estimated power output and decline curves for pressure and temperature based on production rates (Uddenberg 2012). The model also outputs economic results as a subroutine if these related parameters are supplied as input values. For this portion of the feasibility study, SMU's focus was on the reservoir potential and did not include the economic subroutine, which was assessed by NREL via the GEOPHIRES model.

As in the other models run, the LPM code focuses on the initial parameters of the formations: pressure, temperature, volume, and porosity. The intrinsic rock properties are based on the rock type (shale versus sandstone), and the related heat capacity, fluid viscosity, and density. The model allows the user to fluctuate the permeability, production time and flow rates, temperature change, and distance between well bores for production and injection.

Using the equations and code from Uddenberg (2012), SMU calculated the total heat in place (Q_{tot}) (Equation 2) for each formation of interest within the region of interest (A, area), utilizing formation thickness (h), average density (p_{av}), temperature start (T_i), and temperature brine reinjected (T_o). Next the maximum energy output (W_{max}) that is possible was determined based on surface and formation temperature drawdown and length of time (Equation 3). Input variables

include those from Equation 2 plus the efficiency of plant (γ), thermal recovery factor (r), average heat capacity (C_{av}), volume (V), and length of formation (L_f).

$$Q_{total} = A \cdot h \cdot p_{av} \cdot (T_i - T_o) \tag{2}$$

$$W_{max} = \frac{\gamma \cdot r \int p_{av} \cdot C_{av} (T - T_o) dv}{L_f} \tag{3}$$

Comparing data from different fields and rock units highlights the general patterns that can then be used to assess the probability of certain rock properties on or near the Eastman Chemical property to occur and help determine if drilling is appropriate.

Cross-Sectional Model

Three cross-section lines (A-A', B-B', C-C') define the area of most reservoir focus to depict a pseudo three-dimensional model of the reservoir at depths of the Lower Trinity Group and Cotton Valley Group for the 10-km area in Figure 7. The lines overlap within the Eastman Chemical minerals land. The cross sections are extended beyond the 20-km radius to understand the broader geology for the purpose of extrapolation to the nearby power plant facilities. The cross sections connect digital .LAS file formats and well sites with color raster logs for additional ability to digitize the geophysical lines, allowing us to extract additional parameter details for computational purposes.
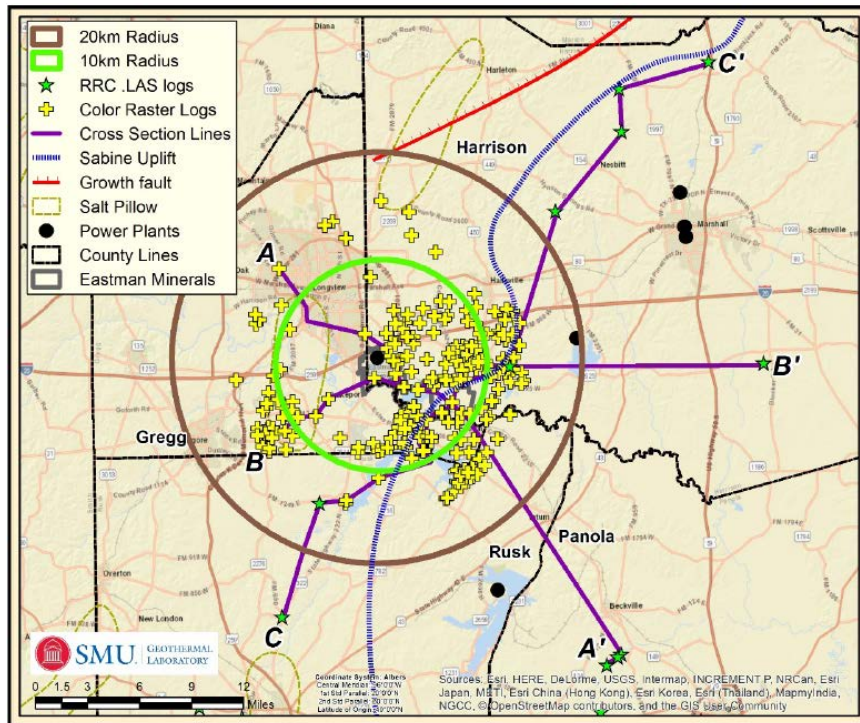
Figure 7. Cross-Section Lines through Wells of Interest. Green stars locate publicly available digital (.LAS) geophysical logs and yellow crosses are well sites with colored raster geophysical logs. These wells of interest were used to determine cross-section lines A-A', B-B' and C-C" that are considered for further evaluation of the possible reservoirs.

In addition to mapping formations for the cross sections, the geophysical logs were used to estimate reservoir properties (porosity, permeability, and water saturation) in a different manner (Tittman 1987). The electrical resistivity, neutron porosity, density, spontaneous potential, and gamma ray logs are used to calculate where there is water (fresh versus salt) and potential for

11

fluid production and injection. This work is an important refining of the reservoir models because the previously mentioned values extracted from publications are specifically for the hydrocarbon zones within the formations. Those oil & gas zones are only a small portion of the total rock volume accessible for fluid production to extract the heat and reinjection of these fluids, and intentionally avoid large water zones, which is the primary target here. Using the full geophysical log is included as a way to calculate the expected reservoir parameter values to extend beyond the perforation zones that are currently published.

1.3 Additional Benefits of Integration with Industrial Facilities

Current geothermal direct-use applications are relatively small capacity, which imposes large project costs for deployment. These project costs include permitting, building stakeholder consensus, and acquiring access to land for drilling and brine transport. Mobilizing resources for a small (typically 1-5 MW_t) installation does not allow the project to develop efficient economies-of-scale. In contrast, the proposed project targets utility-scale natural gas plants that could accept 10s of thermal megawatts for a single installation. Furthermore, these power plant sites are commonly surrounded by large areas of land that is owned or controlled by the site operator, simplifying project access and planning.

One of the challenges with direct-use geothermal systems is variation and intermittency in demand from the user facility, which can impact reservoir properties, utilization, and project economics. The proposed integration approach offers flexibility that can allow for uniform geothermal heat use, even when power generation from the user plant varies. This is accomplished by incorporating an energy storage option in the process, namely chilled water. The process integration is discussed next.

1.4 Turbine Inlet Cooling

An attribute of all combustion turbines is that hot weather decreases power capacity. The impact ranges from 10 percent to 35 percent of the rated/nameplate output capacity, which is rated at 59°F (15°C) as specified by the International Standards Organization. To compound matters, as ambient temperature increases, power demand and electricity prices typically increase too. Thus, turbine output decreases when it is most needed. In combined-cycle, cogeneration and combined-heat-and-power (CHP) systems, a rise in ambient temperature not only reduces the turbine power output, it also reduces the total thermal energy available in the turbine exhaust gases for the desired downstream use. To combat these effects, turbine inlet cooling (TIC) decreases the temperature of the inlet air to increase the gas density, allowing turbine performance to recover.

TIC can be provided by evaporative cooling of the inlet air or through sensible chilling via mechanical vapor-compression or thermal absorption chillers, Figure 8. Evaporative coolers are simpler and less expensive, but these systems are limited by the local wet-bulb temperature and do not work as well in high-humidity regions. Prior studies have shown that active chilling can yield much greater benefits in terms of increased power output (Figure 9), especially in humid climates such as East Texas.
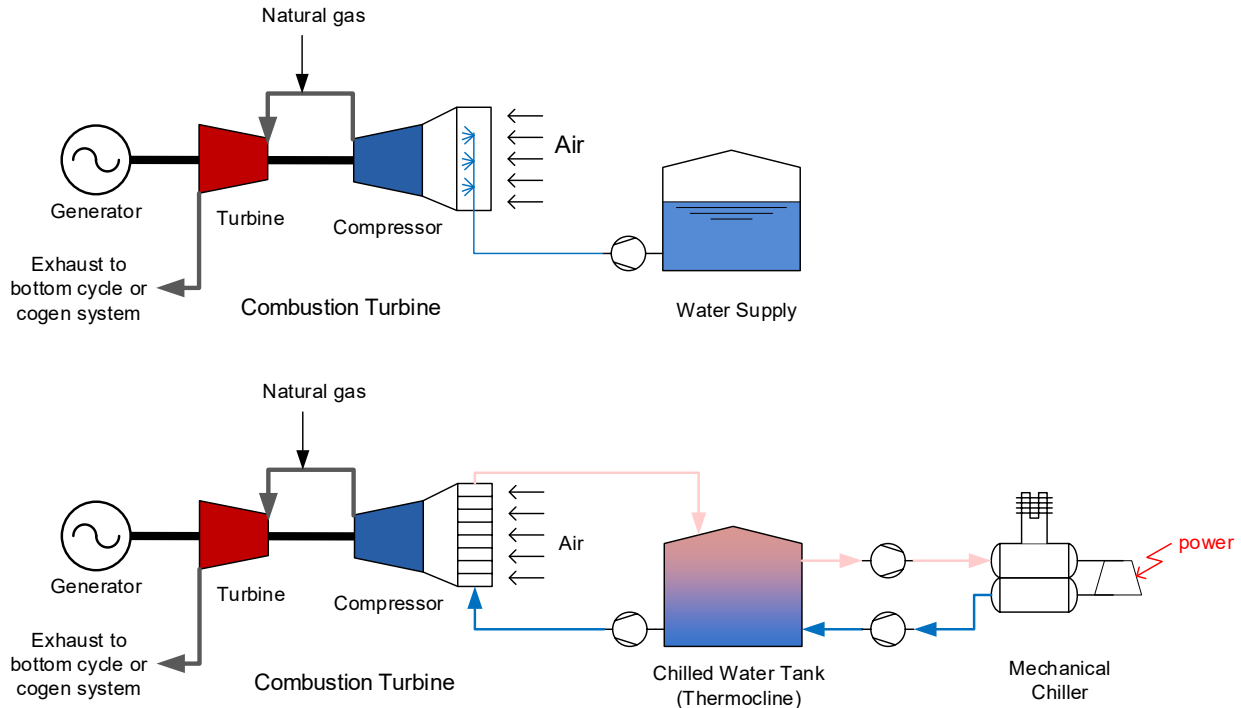
Figure 8. Typical TIC systems - evaporative cooling via spray injection (top) and chilled-water cooling with mechanical chiller (bottom).
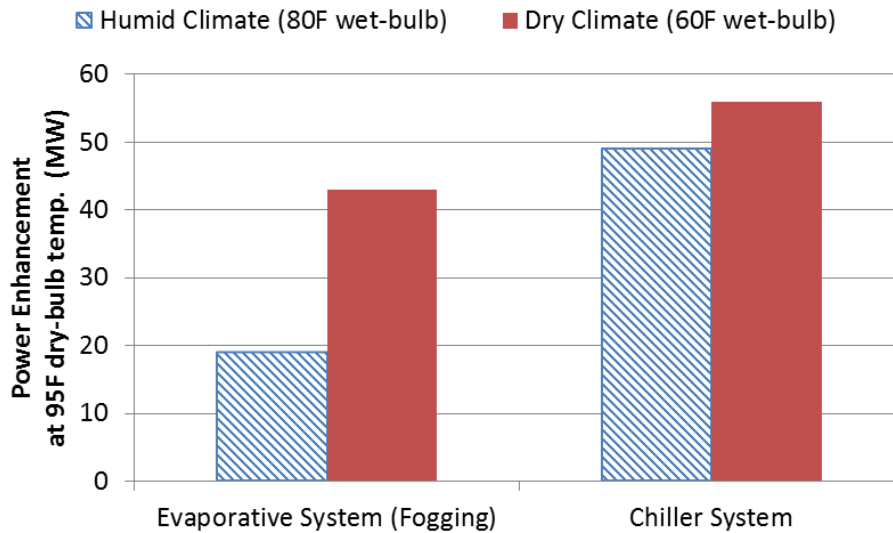
Figure 9. Benefit of TIC as a function of technology and climate. Chiller systems are more beneficial in humid climates, such as found in East Texas and the Gulf Coast (Punwani 2008).

1.5 Absorption Chillers with Thermal Storage

Although not as intuitive as direct heating, geothermal energy can be used to provide cooling using commercial absorption chillers. At reduced pressure, water evaporates at low temperature while absorbing heat and this phenomenon can be used to produce refrigeration. A low-pressure condition is maintained in an evaporator/absorber using a salt solution that has a strong affinity

13

for water (Figure 11). This salt, typically lithium bromide, absorbs water vapor that evolves from the evaporator to maintain the low-pressure condition in the chamber. The diluted salt solution is regenerated by (geothermal) heat and recycled to the absorber (Figure 10). A separate chilled water loop can include storage to decouple the rates of production and use of the chilled water. This chilled water can be dispatched to coincide with the periods of greatest power demand and/or hottest ambient temperatures to ensure the greatest economic benefit for the plant.

Prior studies that explored the use of absorption chillers for TIC identified as a limitation the need to couple heat availability from the operating power plant to the demand for chilling. Integrating geothermal energy removes this constraint, while inclusion of thermal energy storage allows for design of a small-capacity chiller that runs 24/7 off the geothermal resource to fill the storage system, which can be dispatched at a different rate as needed as illustrated in Figure 11.
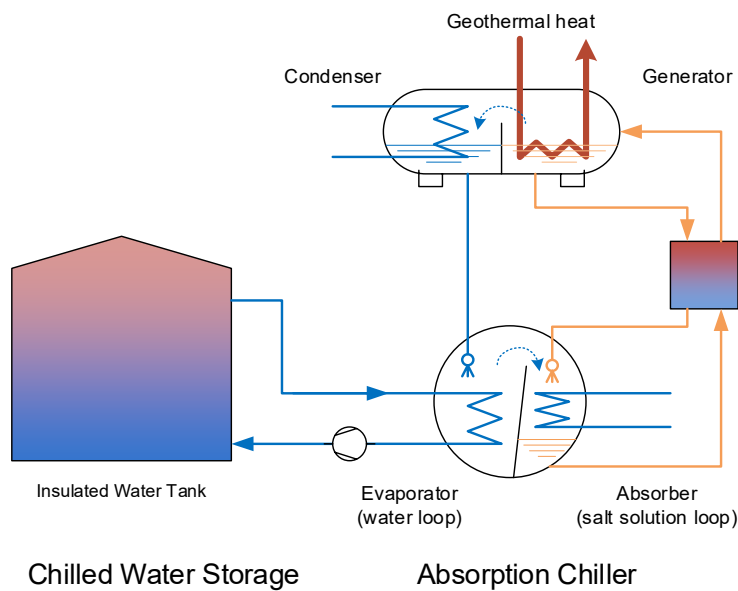
Figure 10. Geothermal heat can be used to generate chilled water via an absorption chiller.
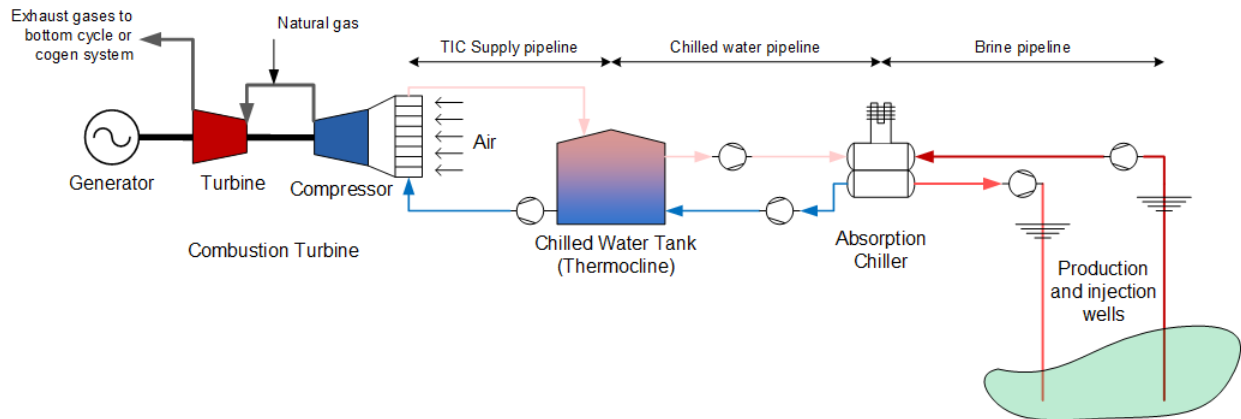
Figure 11. Turbine inlet cooling provided by geothermal-driven absorption chillers. The use of chilled-water storage allows one to decouple the geothermal use from the TIC dispatch.

14

2 Results

2.1 Geothermal Resource Modeling

2.1.1 Geothermal Gradient and Depth to Reservoir Rocks

One of the first steps in calculating heat flow is determining the regional geothermal gradient (°C/km) for the study area (Figure 12). The gradient is from BHT to surface and is smoothed to show trends, which generally increases to the east, corresponding to movement toward the center of the Sabine Uplift with increased heat production and decrease in sediment thickness. The gradient map is a way to confirm that the salt pillows are not influencing the nearby temperatures.
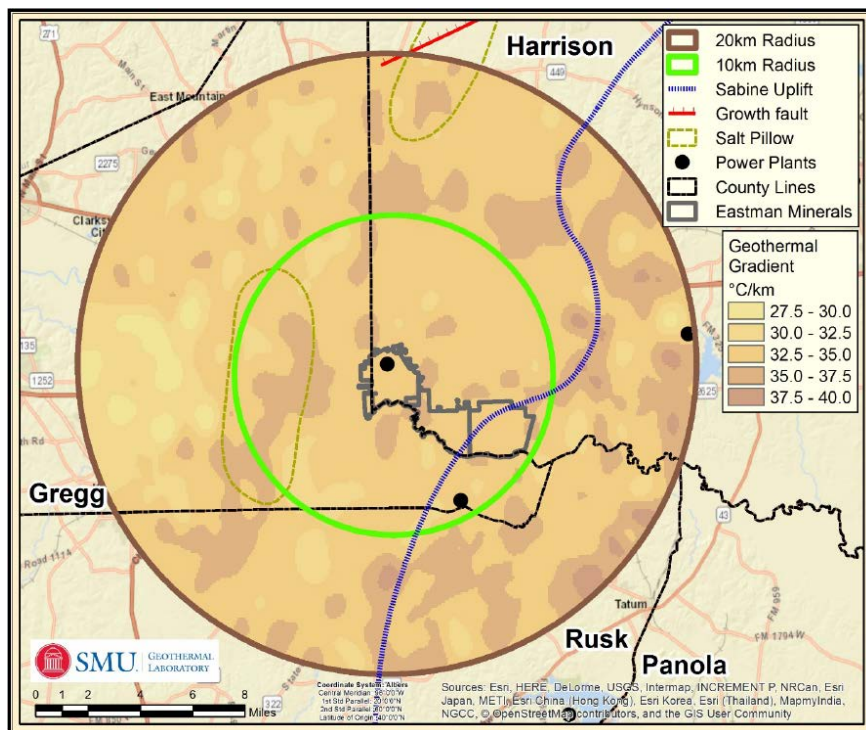
Figure 12. Geothermal Gradient of the Feasibility Study Area. The primary tectonics and salt pillow locations are overlaid on the gradient map. The gradient contour interval is 2.5 °C/km with a general trend of warming to the East.

This geothermal feasibility study is focusing on extractable heat-in-place for DDU rather than electricity generation. Hence, the goal is to determine how much thermal energy is stored within the specific formations of interest and estimate the amount of fluid flow possible. Heat Flow is part of the stored thermal energy determination. The thickness of the primary formations (Pettet, Travis Peak, Cotton Valley, see Figure 4) thicknesses are used to calculate the volume. The Pettet and Travis Peak are considered top candidates for this feasibility study based on their total thickness and production and injection intervals. The Top of the Travis Peak formation deepens to the west (2,300 m) along the 20-km radius circle (Figure 13). This is where the East Texas Basin oil field (the first one in Texas!) is located.

15
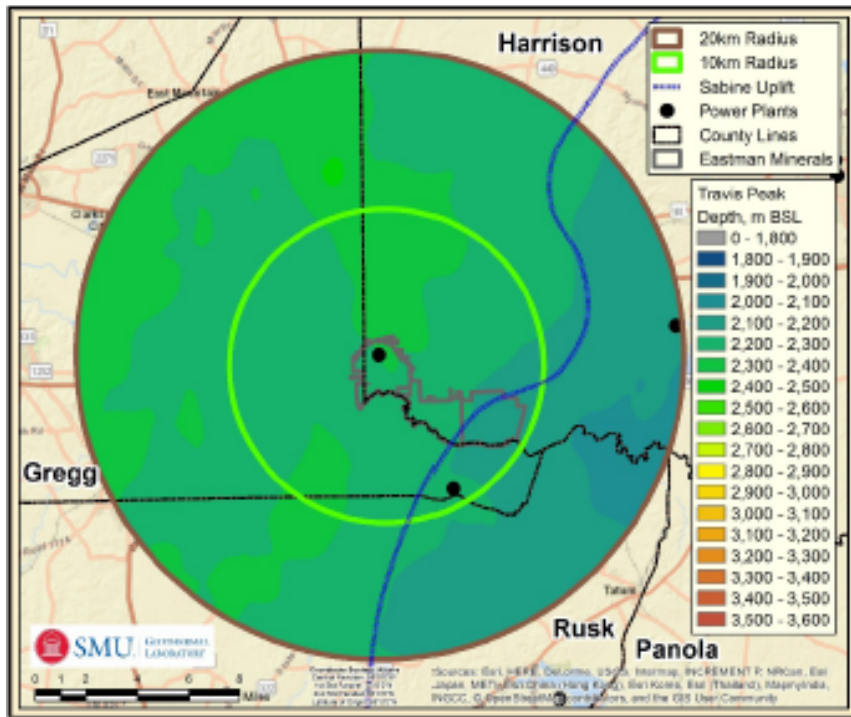
Figure 13. Travis Peak Average Depth to Formation Tops in meters (upper map) Top of the Travis Peak Formation in the NW quadrant is approximately 2,500 m depth then shallows toward the east to 2,000 m depth below sea level.

2.1.2 Reservoir Characteristics

The gas fields in the study region produce from low permeability and porosity zones (Ahr, Steffensen, and Faucette 1984; Becker et al. 2010; Vavra, Sheihling, and Klein 1991). The deeper Cotton Valley formation is typically hotter (from approximately 117 to 130°C), yet permeability is primarily 0.01 to 1.0 mD and porosity less than 12% (Table 2) The shallower Trinity Group (Pettet/Sligo and Travis Peak/Hosston) contains much more variability, 0.01 to 2000 mD permeability and 1 to 23% porosity yet has lower temperatures (approximately 98 to 117°C), as expected with the shallower depths. The shallower formations are considered despite the lower temperature because of increased ability to produce larger volumes of water and extract enough heat before reinjection.

Table 2. Estimated reservoir characteristics based on published well data. Geologic units are in order of depth and age. Thickness is an average based on the difference between formation tops/bottoms (MAX) and injection perforations (AVE) and hydrocarbon productivity zones (MIN).

Geologic Unit Name	Other ID	Porosity (%)	Permeability (mD)	Thickness (m)	RFC	RPI
Pettet Limestone	10 km AVE	14	110	38	4,176	9
	10 km MAX	21	900	100	89,964	200
	10 km MIN	11	4	2	8	0
Travis Peak Sandstone	10 km AVE	13	65	383	24,863	55
	10 km MAX	15	90	550	49,427	110
	10 km MIN	8	15	200	2,984	7
Cotton Valley Sandstone	10 km AVE	7	0	120	30	0
	10 km MAX	12	4	450	1,770	4
	10 km MIN	2	0	25	0	0

16

2.2 Geothermal LCOH Calculation with GEOPHIRES

GEOPHIRES (GEOthermal energy for Production of Heat and electricity ("IR") Economically Simulated), was developed by Massachusetts Institute of Technology to perform techno-economic simulations of geothermal energy systems. In 2018 GEOPHIRES was updated by NREL, as version 2.0, to combine reservoir, wellbore, subsurface parameters (Table 3) and surface plant technical models (Table 4) with cost correlations and levelized cost models to estimate the capital and operation and maintenance (O&M) costs (Table 5), instantaneous and lifetime energy production, and overall levelized cost of energy of a geothermal plant (Beckers and McCabe 2019).

Table 3. GEOPHIRES Model Assumptions: Subsurface Technical Parameters

Subsurface Technical Parameters		
Reservoir Model:	TOUGH2 simulator	
Wellbore Model:	Ramey Wellbore Model	
Reservoir Depth:	2.7	km
Temperature Gradient:	37.5	°C/km
Number of Production Wells:	1	
Number of Injection Wells:	1	
Production Well Diameter:	8.5	inches
Injection Well Diameter:	8.5	inches
Production Flow Rate per Well:	125	kg/s
Injectivity Index:	5.5	kg/s/bar
Productivity Index:	5.5	kg/s/bar
RPI	55	kg/MPa-s
Injection Temperature:	88	°C
Reservoir Heat Capacity:	1000	J/kg/K
Reservoir Density:	2750	kg/m^3
Reservoir Thermal Conductivity:	3.48	W/m/K
Reservoir Porosity:	15	%
Reservoir Permeability:	6.50E-13	m^2
Reservoir Thickness	383	m
Reservoir Width:	1000	m
Well Separation:	1000	m

Table 4. GEOPHIRES Model Assumptions: Surface Technical Parameters

Surface Technical Parameters		
End-Use Option:	Direct-Use Heat	
Circulation Pump Efficiency:	0.8	
Capacity Factor:	0.9	
End-Use Efficiency Factor:	0.9	
Surface Piping Length:	5	km
Surface Temperature (ground):	20	°C
Ambient Air Temperature:	20	°C

17

Table 5. GEOPHIRES Model Assumptions: Economic and Financial Parameters

Economic and Financial Parameters		
Economic Model:	Standard LCOH model	
Plant Lifetime:	30 years	
Discount Rate:	5	yr
Inflation Rate:	0	%
Well Drilling and Completion Capital Cost Adjustment Factor:	1.05	
Well Drilling Cost Correlation ($, d=depth in meters):	0.1371*d² + 129.6*d + 1205600 ‡	
Reservoir Stimulation Capital Cost Adjustment Factor:	0	
Surface Plant Capital Cost Adjustment Factor:	0	
Field Gathering System Capital Cost Adjustment Factor:	1	
Pipeline Distribution Capital Cost Adjustment Factor:	1	
Exploration Capital Cost Adjustment Factor:	1	
Wellfield O&M Cost Adjustment Factor:	1	
Surface Plant O&M Cost Adjustment Factor:	0	
Water Cost Adjustment Factor:	1	
Electricity Rate:	0.07	$/kWh

‡ See note below regarding the well drilling cost correlation.

In addition to electricity generation, direct-use heat applications and combined heat and power or cogeneration can be modeled. GEOPHIRES v2.0 includes various upgrades, including: updating the built-in cost correlations, coupling to the external reservoir simulator TOUGH2 (Pruess, Oldenburg, and Moridis 1999), enhancing the built-in wellbore simulator, converting the programming language to Python, and making the code open source (Beckers and McCabe 2019). GEOPHIRES v2.0 has three built-in models to calculate Levelized Cost of Heat (LCOH).

- Fixed Charge Rate (FCR) Model
- Standard Levelized Cost Model
- BICYCLE Model

The present study used the standard levelized cost model:

$$LCOH = \frac{C_{cap} + \sum_{t=1}^{LT}\frac{C_{o\&m,t}}{(1+d)^t}}{\sum_{t=1}^{LT}\frac{E_t}{(1+d)^t}} \tag{5}$$

C_{cap} : total upfront capital investment (M$)
$C_{o\&m}$: average annual O&M cost (M$/yr)
d : real discount rate [5%]
LT : plant lifetime (years) [30 years]
E : average annual net amount of heat produced (MMBtu, MMBtu = million Btu)

GEOPHIRES considers the following categories to estimate capital cost:

- Exploration cost
- Drilling cost with well completion
- Field gathering system
- Surface equipment cost

Built-in cost correlations incorporate indirect costs and contingency. Changes in this study from the GEOPHIRES default values include:

- Exploration costs were kept at the GEOPHIRES default value, which may over-estimate their costs in this application, given the existing data on the regional resource. This possibility was accommodated by later sensitivity runs that varied exploration costs (discussed in Section 2.5).
- Selection of the TOUGH2 reservoir model
- Adjusted drilling costs for regional experience. Team discussions with experts in the study region indicated that drilling costs were lower than the default assumptions in GEOPHIRES. Six cost estimates were obtained and the results corresponded more closely to the "small diameter, vertical open hole Intermediate 1" scenario from (Lowry et al. 2017), Figure 6, which was subsequently used in this analysis.
- Surface equipment costs set to zero (calculated outside of GEOPHIRES)
- Discount rate lowered to 5% (from default 7%)

GEOPHIRES considers the following categories to estimate annual O&M cost:

- Well Field O&M Cost: The built-in correlation for the wellfield O&M costs consists of 1% of the total drilling and field gathering system costs (for annual non-labor costs) and 25% of the labor costs.

- Average Annual Pumping Cost: Includes power consumption for the geothermal fluid production and circulation pumps at the user-provided electricity rate (0.07 $/kWh).

- Plant O&M Cost: Consists of 1.5% of the total plant capital cost (for annual non-labor costs), and 75% of the annual labor costs. Plant costs are estimated in the Chiller and Turbine Inlet Cooling cost model

Changes in this study from the GEOPHIRES default values include:

- Surface plant O&M costs set to zero and calculated outside of GEOPHIRES

2.3 Modeling the Power Plant

A model of the host site's co-generation plant was developed in IPSEpro—a process simulation tool developed by SimTech that calculates heat balances and predicts design and off-design performance of power-plant components and systems. The combined-cycle power plant consists of two General Electric PG7241(FA) gas turbines (GTs) each with a rated capacity of 171.7 MW$_e$. Each turbine exhaust is linked to a Heat Recovery Steam Generator (HRSG), and a fraction of the hot steam powers a single two-stage steam turbine with a rated capacity of 126.5 MW$_e$ (Figure 14). The remaining steam is used in the chemical plant processes. This process steam is then returned to the power block, and its remaining enthalpy is used to heat the GT fuel, and then to pre-heat the inlet water to the HRSGs (Figure 15). Steam is also extracted from the high-pressure (HP) turbine stage for use in the chemical plant.

This report is available at no cost from the National Renewable Energy Laboratory at www.nrel.gov/publications.
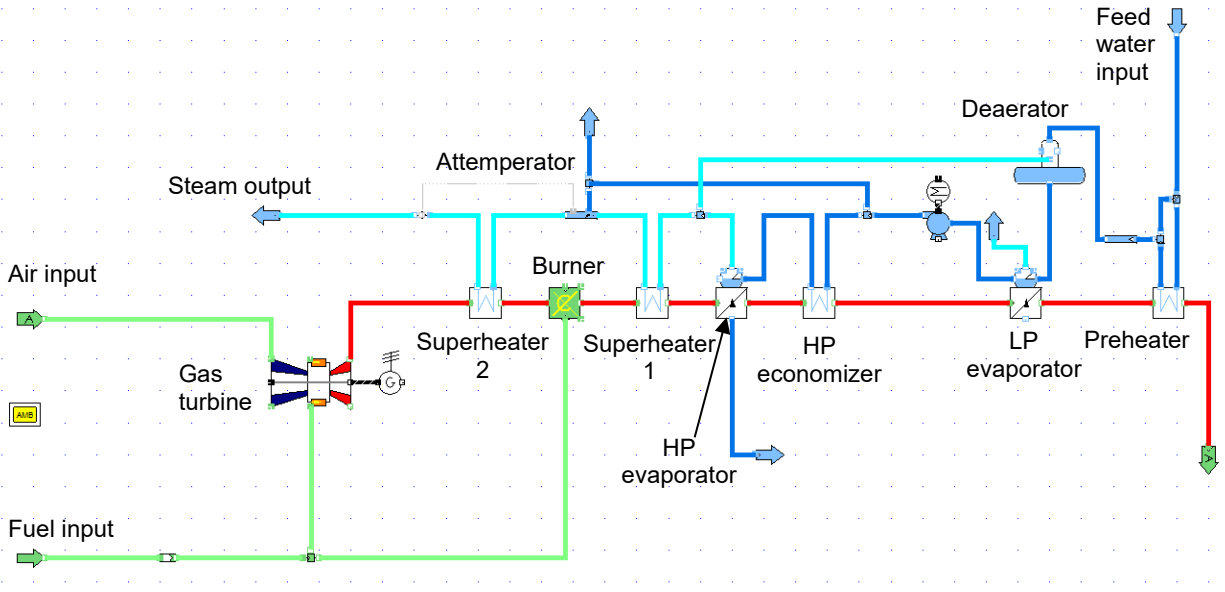
Figure 14. Screenshot of a single gas turbine and heat recovery steam generator model from the simulation software IPSEpro. The actual plant has two GT/HRSG pairs that supply steam to a single steam turbine as well as the chemical plant.

The host site provided process flow diagrams and design specification sheets for the gas turbines, steam turbine, and HRSGs to aid the analysis. These data specify the temperatures, pressures, and mass flow rates around the cycles, as well as the power output. This information was used to develop design and off design models of the system in IPSEpro.
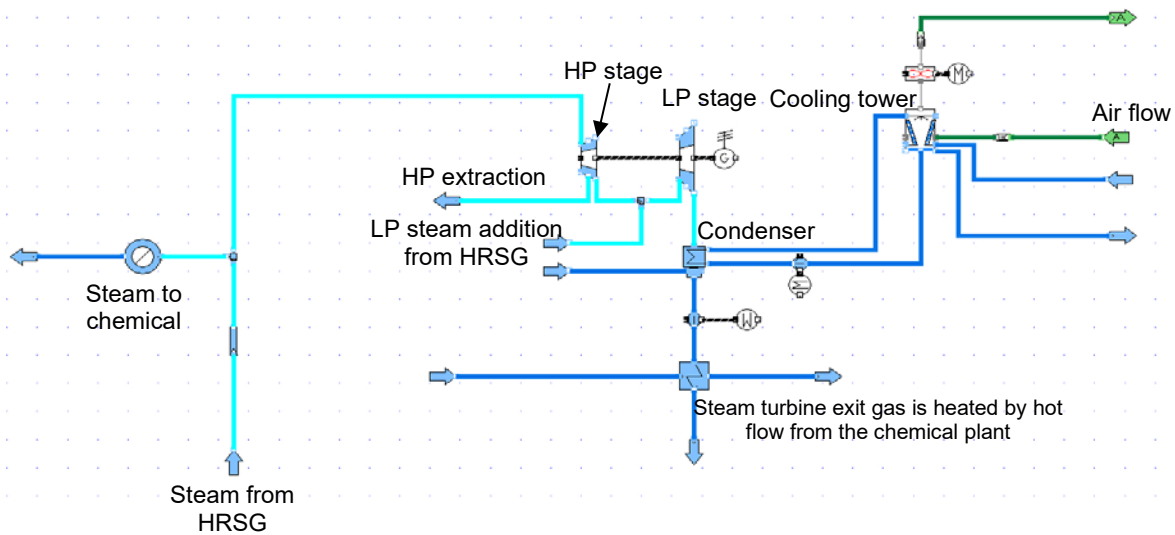
Figure 15. Screenshot of the steam turbine cycle from the simulation software IPSEpro.

The response of the system to variations in ambient temperature and load were investigated to understand the system's off-design behavior. Modeling the full system (gas turbines, steam turbines, and HRSGs) led to problems with the model convergence when the system was far from the design point. Therefore, it was decided to model the gas turbine separately from the

20

steam turbine. This allowed a wider range of off-design operational points to be investigated. This approach is justified because the gas turbine cycle and steam turbine cycle are not strongly coupled to one another; that is, the exhaust gas from the gas turbine does not directly correlate with the steam inlet flow to the steam turbine. This is a result of the variable steam demand of the chemical plant. The operational data indicated that steam entered the steam turbine at a constant temperature and pressure. The steam mass flow rate did not depend directly on the steam generated in the HRSG because the quantity of steam sent to the chemical plant varied significantly. Therefore, it is possible to model the gas turbine separately from the steam cycle. These individual models were used to develop correlations relating the power output, mass flow rates, and ambient temperatures.

Operational data for the cogeneration plant was provided for 15-minute intervals for six representative days in 2017. The operational data included power generation, air mass flow rates, fuel flow rates, wet-bulb and dry-bulb temperatures and pressure. For each hour, the relative humidity, specific humidity and enthalpy were calculated. The operational data were used to validate the design and off-design IPSEpro model. The normalized heat rate is plotted versus part load fraction in Figure 16. Heat rate (fuel thermal content divided by electric generation, MMBTU/kWh) is a common measure of fossil-power cycle efficiency. Data in Figure 16 are shown for both gas turbines along with ±5% error bands. Model agreement was within ±5%. Interestingly, the two turbines have slightly different operational performance, as is illustrated in Figure 17. For a given power output, gas turbine 2 (GT2) requires a larger flow of air than GT1. GT1 reportedly received maintenance more recently than GT2 which may account for this difference. As a result, the two gas turbines are modeled separately with different correction curves, so that IPSEpro can accurately capture the two scenarios.
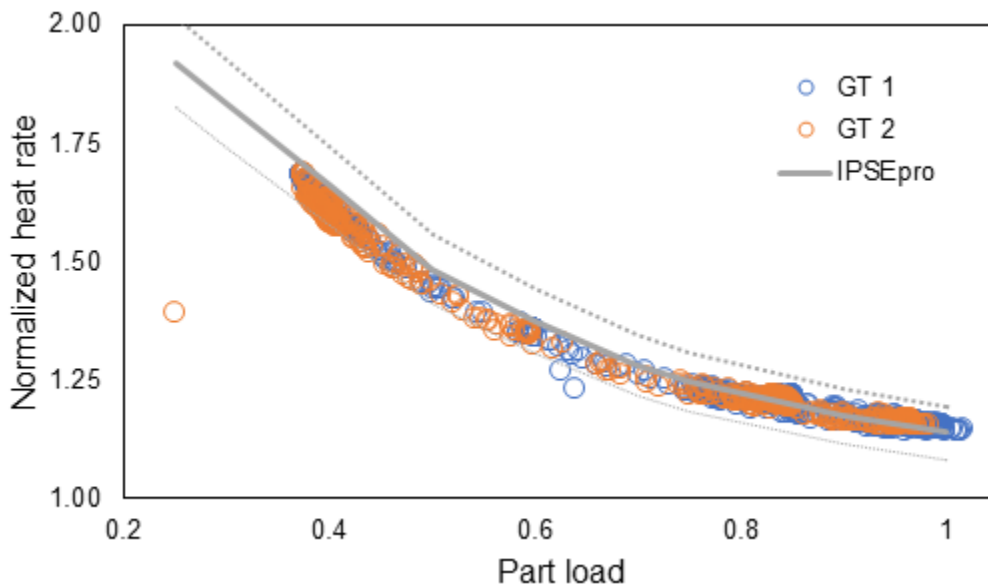
Figure 16. Variation of heat rate with part load operation for the gas turbines. This figure compares operational data and IPSEpro model output. The model heat rate ±5% is illustrated with dotted lines.
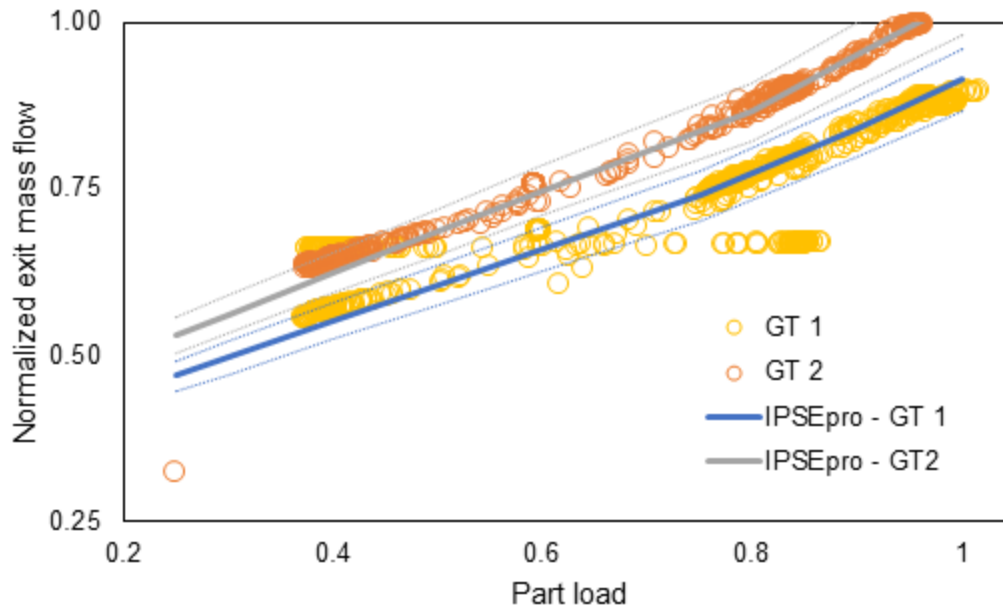
Figure 17. Variation of exhaust mass flow with part load operation for the gas turbines. This figure compares operational data and IPSEpro model output. A model flow rate ±5% is illustrated with dotted lines.

The steam turbine behavior is illustrated in Figure 18 with error bounds of ±5 % on the modeled results. The steam data show greater variability, which is indicative of the varying steam usage by the chemical plant. Greater variation in the steam data is not viewed as detrimental to the project analysis because most of the benefit from turbine inlet cooling occurs within the gas turbine. Having developed and validated the IPSEpro simulation model, the team could then apply the model to estimate the performance impact of different TIC scenarios.
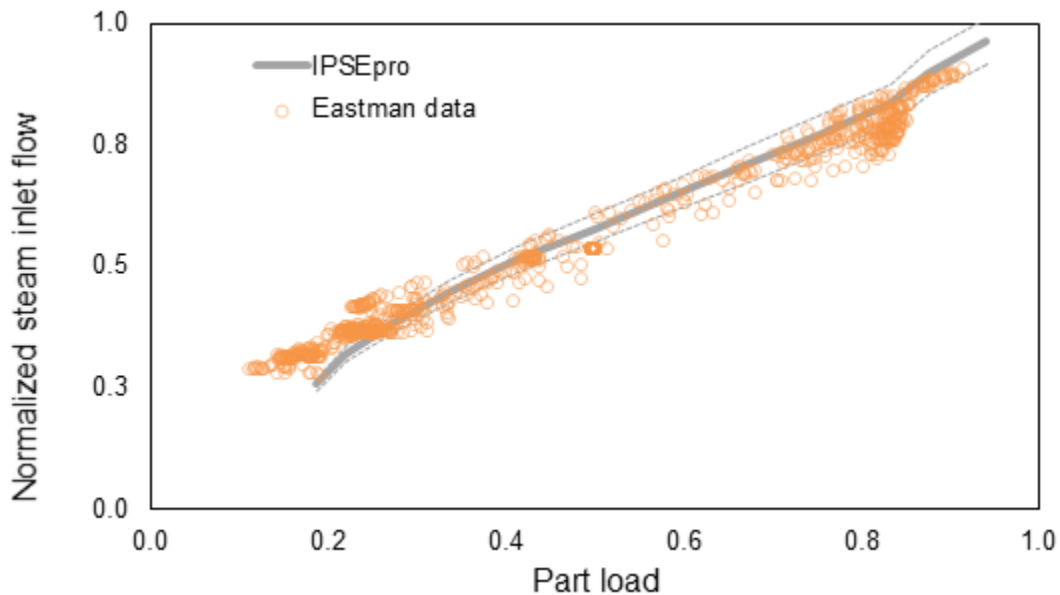
Figure 18. Variation of steam inlet mass flow with part load operation for the steam turbine. This figure compares operational data and IPSEpro model output. The model flow rate ±5% is illustrated with dotted lines.

22

2.4 Integrated TIC System Simulation

The turbine inlet cooling system comprises an absorption chiller and storage vessel (Figure 11) that is filled from the chiller. The chiller is assumed to run at full load for the entire year off geothermal energy. The *available cooling* at each hour is the cooling that can be supplied by the storage tank down to a minimum value equal to the capacity of the chiller. The specific *cooling opportunity* is given by the difference in enthalpy between the observed value of the inlet air properties and the desired gas turbine design-point value[1].

Storage provides a way for the geothermal system and chiller to run at full load all year, thereby meeting a flexible cooling demand while reducing the size of these components. The optimal sizing of the chiller and storage, and the storage dispatch strategy are closely related and require careful analysis. For example, a 12-MW$_t$ chiller at the Eastman plant could provide about 80% of the annual cooling opportunity with no storage Figure 19 (top). The chiller provides more than enough cooling throughout the winter. However, summer cooling loads frequently exceed 12 MW$_t$ and the chiller rarely cools the air to the design value. However, it is notable that the chiller can generate an annual total of 105.1 GWh$_t$ of cooling energy, while annual cooling opportunity is only 60.3 GWh$_t$. This indicates that the chiller is large enough (perhaps too large), but that it cannot always provide cooling at the required times. Storage can provide the flexibility to deliver cooling independent of the chiller status and provide greater cooling power than the chiller can on its own.

The influence of a 5000 m^3 (1.3 million gallons) storage tank on the delivered cooling is shown in Figure 19. By filling the storage when cooling opportunities are low, it is possible to meet the cooling opportunity for much of the summer. There is a notable period in the summer where the cooling opportunity is above the chiller load for several days. As a result, the storage is not filled during this period, and the maximum cooling that can be delivered is 12 MW$_t$.

---

[1] The design point conditions are a dry-bulb temperature of 15°C and a relative humidity of 60% (corresponding to a dry-bulb temperature of 10.8°C).
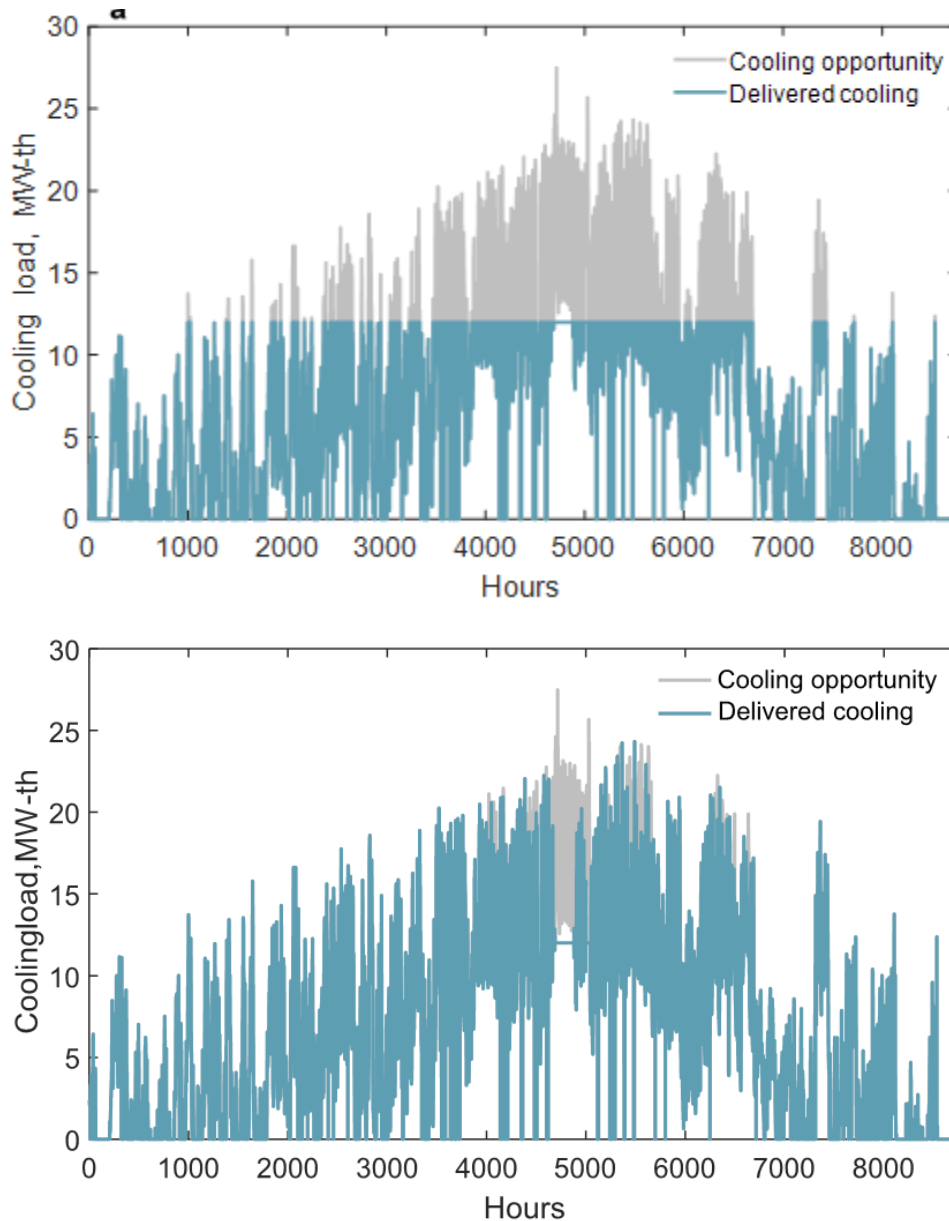
Figure 19. The hourly cooling load that is required, and the cooling load that is supplied to the Eastman co-generation plant with a 12-MW$_{th}$ chiller: (top) No storage, (bottom) with 5000 m^3 storage.

In the initial analysis, the dispatch of cooling water is controlled in a simple fashion:

- If the cooling opportunity is less than the cooling power of the chiller, the turbine inlet air is cooled to the design value, and excess cold water fills the tank. If the tank is full, the chiller capacity cannot be used and is bypassed.
- If the cooling opportunity is more than the cooling power of the chiller, the chilled water level in the tank falls as it is dispatched. Once the storage tank is emptied, the available cooling is equal to that supplied by the chiller. The turbine inlet air temperature is then calculated from the cooling that is available.

24

Having evaluated the temperature of the inlet air after cooling, the new power output for that hour may be found from the correlation developed with IPSEpro. The method above can use different dispatch algorithms, from very simple to sophisticated assessments of the market and weather conditions. The first, simplest model assumed dispatch whenever chilled water is available and cooling potential exists. More sophisticated dispatch algorithms were used in the later technoeconomic assessment.

Figure 20 illustrates representative simulation results with a 12 MW$_t$ chiller and a 5000 m^3 storage tank. The results indicate TIC can provide a 10-25% increase in power output during afternoon summers, which met the project's metric that required showcasing the ability to increase plant power by at least 10%. This performance model is next used for a techno-economic assessment of the proposed application.
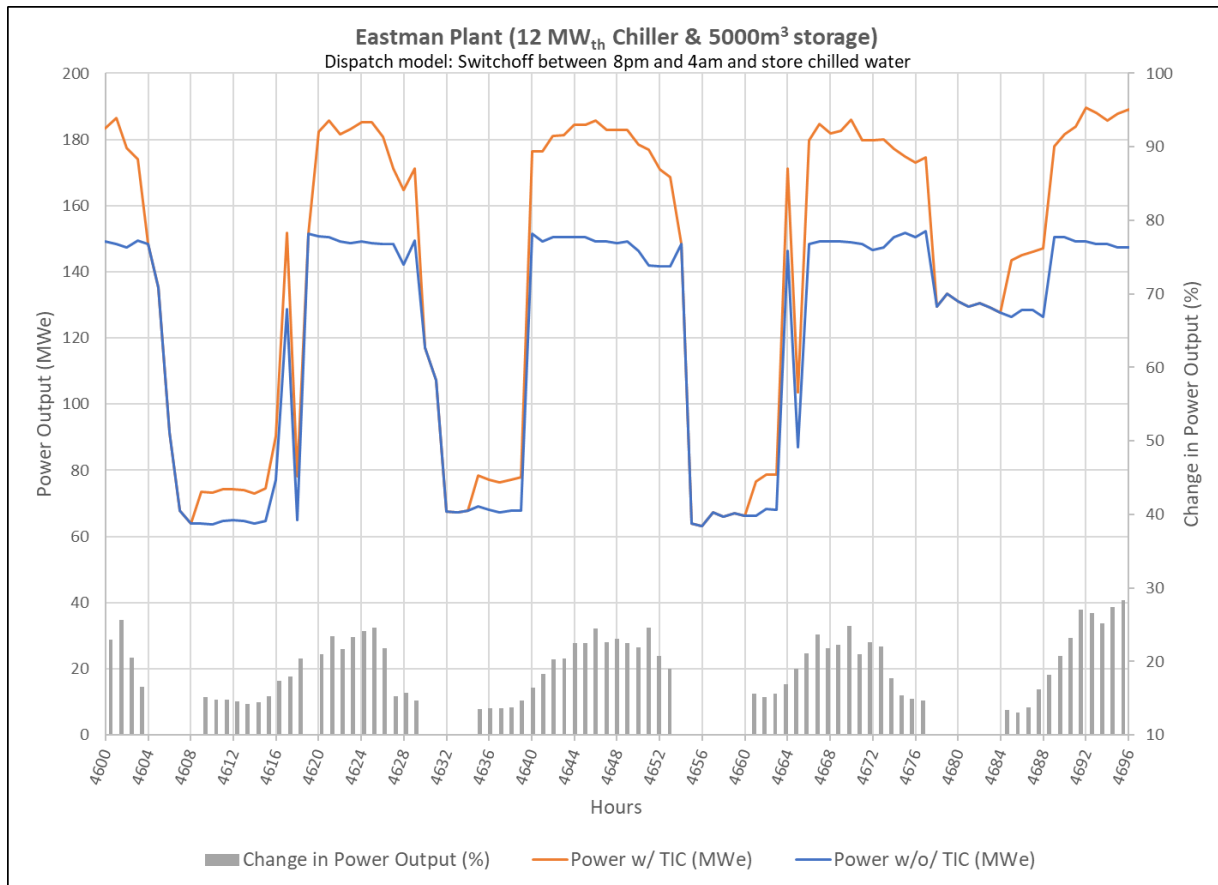
Figure 20. Increased power output exceeds 20% during summer afternoons with TIC, thereby meeting the metric of project Milestone 2.3.

25

2.5 Techno-Economic Assessment

2.5.1 Simple Payback Period

A system schematic for the proposed geothermal integration for TIC is provided in the Appendix. This representation shows the configuration and capacities for a hypothetical TIC system at the Eastman Chemical plant in Longview, TX. The geothermal source is based on the conditions defined by the SMU analysis of the region and extraction of geothermal energy from the Travis Peak Sandstone formation (Batir, Richards, and Schumann 2018). The capacities and operating conditions for the gas turbine and steam turbine systems are derived from the Eastman co-generation plant. That unit is a "2-on-1" combined cycle plant, with two largely identical gas turbines, each feeding a heat recovery steam generator (HRSG) to produce steam that is used by the steam turbine or exported to the chemical plant. Duct burners are available to allow gas combustion to produce additional steam. Returning steam from the chemical plant and steam turbine is condensed using evaporative cooling towers. This system was modeling by NREL within IPSEpro as described in the prior section.

The year 2017 was selected for the techno-economic analysis because the team had weather data, plant operating data, power market and natural gas cost data for that year. Climate data for the site was acquired from Eastman Chemical and hourly real-time electricity price data for 2017 were obtained from the Southwest Power Pool (https://www.spp.org/)—the wholesale power market in which the plant resides. The additional income is found by multiplying the additional power output by the locational marginal price at each hourly timestep. Daily natural gas prices for the Houston Ship Channel were obtained for 2017 to allow calculation of additional fuel cost when TIC is operating. The net annual revenue (effectively the operating profit from TIC) is the expenditure on natural gas and system O&M subtracted from the additional electricity sales revenue. Hence, overall economics depend on optimizing the dispatch of chilled water based on weather conditions and market power prices.

TIC requires an increase in fuel consumption in proportion to the increased power, while at the same time improving gas turbine heat rate (El-Shazly 2016). Discussion with TAS indicates that the gas turbine heat rate typically decreases slightly, ranging up to 2%, but more typically around 1%. TAS provided a rule-of-thumb for TIC applications that a 10% increase in power output would incur a 7% increase in fuel consumption. Heat rate is inversely related to plant efficiency and is defined as the ratio of fuel consumption to electric power generation. Hence, a decrease in heat rate is an increase in efficiency. In this situation the heat rate "improvement" results from maintaining heat rate near its design-point value, rather than it decreasing with ambient temperature (El-Shazly 2016); nonetheless, the net effect is better heat rate with TIC. (Note that this improvement affects the entire turbine output, not just the additional power provided under TIC.) Fuel costs are the major operating expense for the gas turbine and the importance of this efficiency improvement is highlighted in Figure 21.
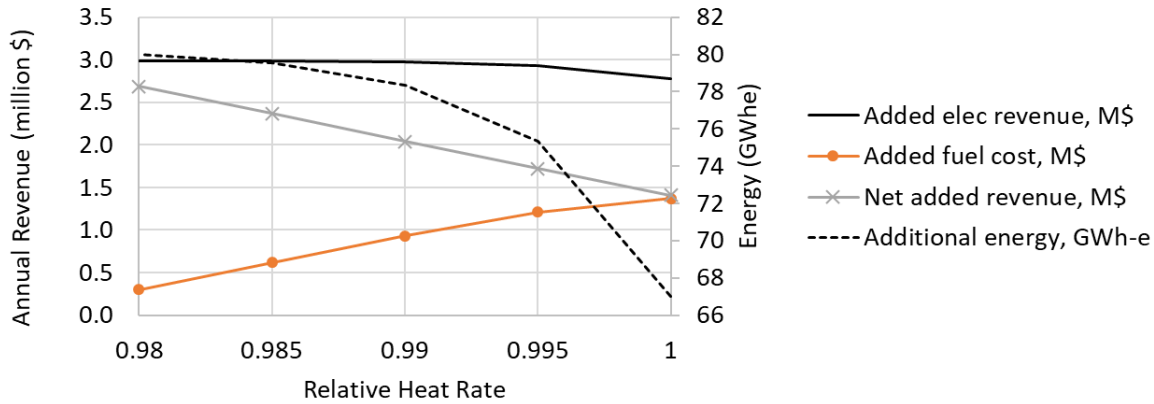
Figure 21. Influence of heat rate improvement on net revenue during TIC.

NREL presented a preliminary economic analysis at the Geothermal Resources Council 2018 meeting (Turchi et al. 2018) that used a simple payback estimate to evaluate overall economics:

$$\text{Simple payback} = \frac{CAPEX}{Annual\ Revenue - OPEX} \text{ (years)}$$

The simple payback analysis utilized capital and operating expense values (CAPEX and OPEX) from industry partner TAS. An example case for a 12-MW$_t$ chiller system with a 5000-m^3 storage tank is shown in Table 6. The TIC System CAPEX values from TAS were $19.0 million for a retrofit plant (such as the Eastman Chemical case) and $13.2 million for a greenfield merchant plant design, resulting in total CAPEX estimates of about $32 million and $27 million, respectively (Table 6).

27

Table 6. Example system cost for geothermal-heat absorption chillers with TIC.

	Eastman Plant	Merchant Plant	Source
Equipment			
TIC Absorption Chillers (12 MW$_t$)	$3,740,600	$3,740,600	TAS
TIC Heat Exchanger (19 MW$_t$)	$2,324,600	$2,324,600	TAS
TIC retrofit kits	$2,025,700	-	TAS
Storage Tank (5000 m^3)	$1,666,000	$1,666,000	EconExpert Installed cost
Shipping & Installation			
Shipping	$202,300	$151,600	TAS (TIC Equipment) * 2.5%
Field Installation	$4,045,400	$3,032,600	TAS (TIC Equipment) * 50%
Retrofit Premium	$2,022,700	$0	TAS
Total Installed Equipment	$16,027,300	$10,915,400	
EPC			
Engineering	$731,800	$579,800	TAS (Equipment) * 7.5%
Start-Up	$243,921	$193,300	TAS (Equipment) * 2.5%
EPC Overhead	$975,700	$773,100	TAS (Equipment) * 10%
EPC Contingency	$487,800	$386,600	TAS (Equipment) * 5%
EPC Margin	$487,800	$386,600	TAS (Equipment) * 5%
Subtotal EPC	$2,927,000	$2,319,400	
Subtotal TIC System	$18,954,300	$13,234,700	
Geothermal System Cost	$13,510,000	$13,510,000	GEOPHIRES
Total CAPEX	**$32,464,300**	**$26,744,700**	
OPEX (Annual)			
Geothermal System	$370,000	$370,000	GEOPHIRES
Chiller & HX	$104,600	$104,600	TAS
Storage Tank	$1,700	$1,700	TAS
Natural Gas Cost	$856,100	$1,229,000	Dispatch model, HR=0.99
Total OPEX	**$1,332,400**	**$1,705,300**	
Additional Power Revenue	**$2,074,200**	**$3,307,700**	Dispatch model

Geothermal system cost, for example, as reported in Table 6, was estimated using GEOPHIRES. The cost for geothermal heat to drive an absorption chiller is summarized by plotting LCOH as a function of the available ΔT, which is defined as the differential between the geothermal resource and the chiller hot water outlet temperature (Figure 22). The chiller outlet temperature is defined by the minimum temperature of the hot water (i.e., brine) leaving the chiller's generator. The assumed chiller outlet temperature for this case study is 88˚C (EPRI 2011). Thus, one can calculate the geothermal resource temperature by adding 88˚C to the ΔT on the x-axis in Figure 22. The delivered geothermal power is also shown. CAPEX is estimated by GEOPHIRES for these cases. Figure 22 emphasizes the importance of maximizing the ΔT for this application, either by locating a hot geothermal source or by reducing the generator outlet temperature in the chiller. The net effect in either case is extracting more energy from the brine.
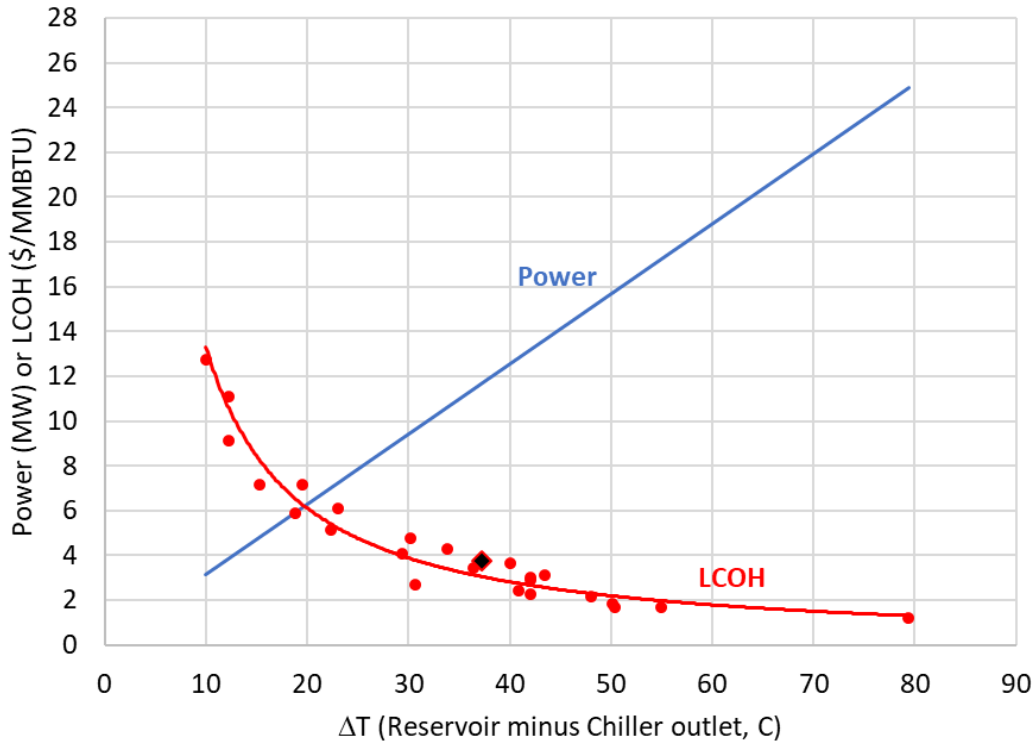
Figure 22. Geothermal thermal power and LCOH for varying temperature differential between the available reservoir and the chiller outlet temperature of 88 ˚C. Each data point represents a different case run in GEOPHIRES. The black diamond indicates the best guess conditions for geothermal CAPEX and reservoir temperature in the Longview, TX region with RPI = 50 kg/MPa-s.

Geothermal LCOH values are sensitive to RPI with increase in RPI values yielding lower LCOH values (Figure 23). For this case study location, SMU's expected RPI (55 kg/MPa-s) yields LCOH ≈ $3.7/MMBTU.
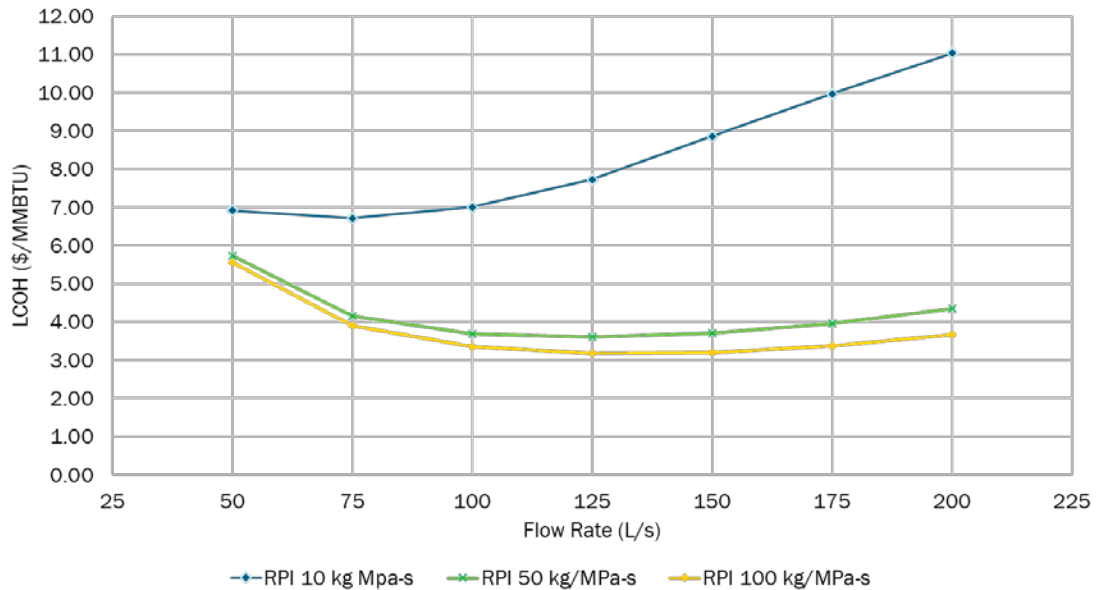
Figure 23. Calculated LCOH values for upper, lower and median RPI values. *SMU expected RPI (55 kg/MPa-s) yields LCOH ≈ $3.7/MMBTU. LCOH shown here does not include the surface plant costs.*

The calculated simple payback time for the Eastman plant and merchant plant scenarios as a function of geothermal LCOH is shown in Figure 24. These values are updated from (Turchi et al. 2018). The chart shows predictions for the Eastman plant based on its 2017 operating profile and a hypothetical merchant plant that operates with a higher overall capacity factor. The greater operating hours of the merchant plant result in shorter payback periods for the TIC and geothermal investment.

Industrial users generally require payback periods of five years or less. However, even in the limit of geothermal heat at LCOH = 0, the estimated payback time for each case exceeds the five-year target, and a more realistic geothermal LCOH target of $3.7/MMBTU yields payback period of 16 years for the merchant plant case. The better economics of the merchant plant highlight the importance of operating at a higher capacity factor.

This report is available at no cost from the National Renewable Energy Laboratory at www.nrel.gov/publications.
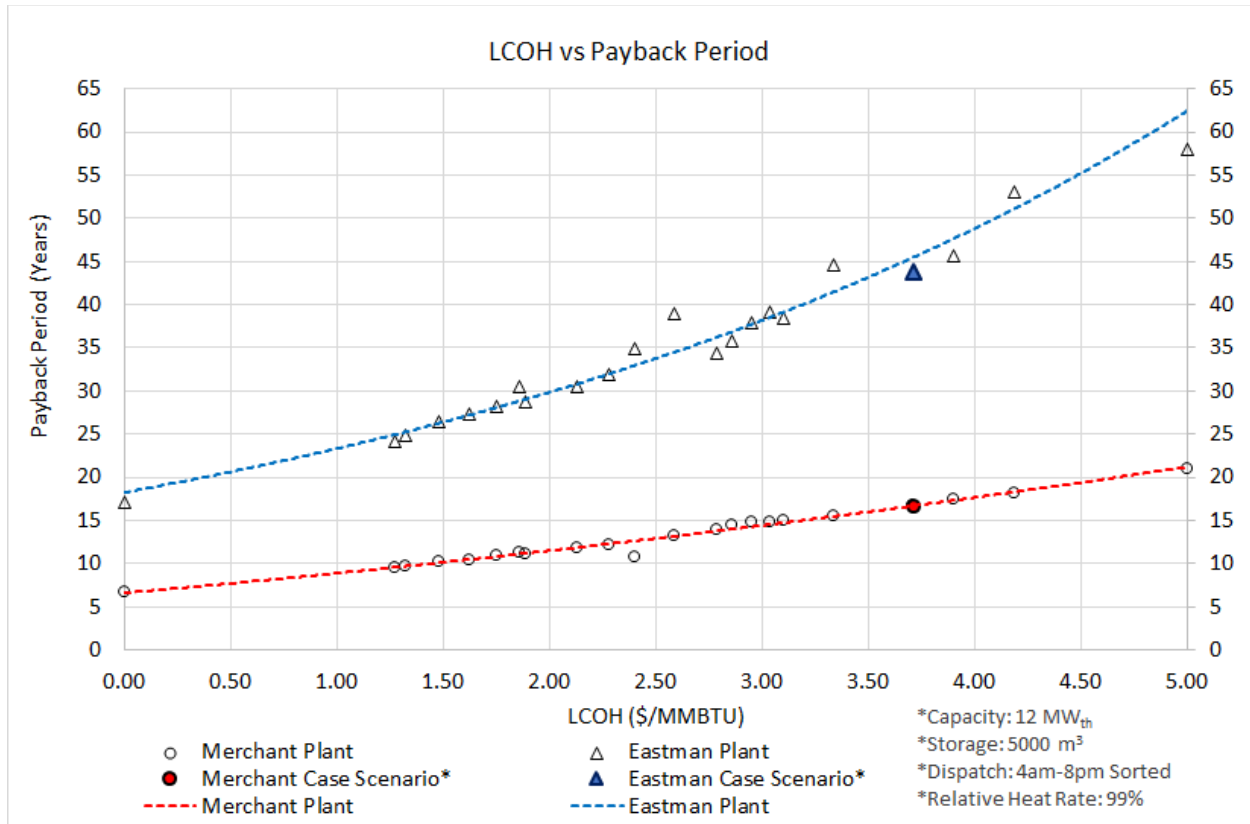
Figure 24. Simple payback time as function of geothermal LCOH for the Eastman and merchant-plant scenarios.

2.5.2 Sensitivity Analysis and Net Present Value Calculations

The final analysis explored the sensitivity of net present value to the sizing of the TIC components and chilled-water dispatch logic. The system capacities that are varied are chiller capacity (MW_t) and chilled water tank volume (m^3). The use of chilled water for TIC provides benefit by increasing power output. Because TIC consumes additional fuel to produce additional energy, it is essential to run the system only when electricity pricing is attractive. At a minimum, the operating (i.e., fuel) cost for the TIC system must not exceed the revenue obtained by the additional electricity sales. Hence the operating logic to decide when to dispatch the TIC is a key variable, and this decision process depends on weather conditions, state of chilled water tank level, and electricity pricing.

The simplest dispatch algorithm for TIC delivers stored cold water whenever opportunity exists. However, it is expected that a more sophisticated control strategy could make better use of the storage to take advantage of the variations in electricity prices (Cole et al. 2014). Figure 25 shows the reported distribution of electricity prices for each hour of the day for 2017. It is notable that prices fluctuate more significantly during daytime hours, and that variations are minimal between 8 pm and 4 am. A better dispatch model would avoid any cooling during these low-value hours and instead fill the storage tank to be available to provide cooling during more profitable hours.

This report is available at no cost from the National Renewable Energy Laboratory at www.nrel.gov/publications.
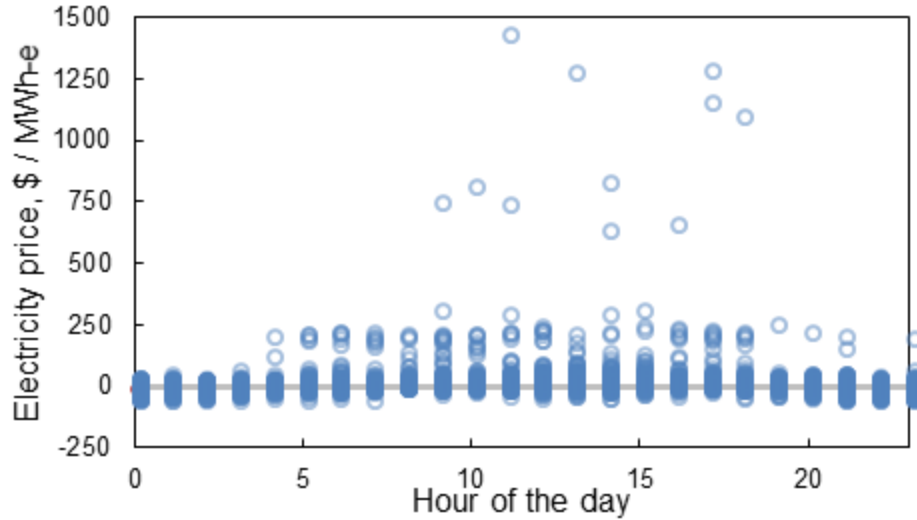
Figure 25. The distribution of electricity prices at each hour of the day for 2017 Southwest Power Pool, south hub locational marginal price.

Preliminary analysis determined that the range of interest in chiller and tank capacities was about 6 to 12 MW$_t$ and 1000 to 10,000 m^3, respectively. (Note that geothermal heat demand is about 30% greater than the chiller capacity to account for chiller efficiency.) Figure 26 illustrates the increasing revenue that is possible by increasingly sophisticated dispatch algorithms. Two cases are shown: (1) the Eastman plant with a 6 MW$_t$ chiller and 5000 m^3 tank, and (2) a comparable size merchant plant with a 9 MW$_t$ chiller and 5000 m^3 tank. The Eastman plant follows the operating status of the facility in 2017, while the merchant plant is assumed free to operate at maximum capacity and represents a best case for the market. Furthermore, two relative heat rates are shown for each plant—a conservative no change (HR100%) and a 1% reduction during TIC (HR99%)—and profits are substantially higher when such a heat rate reduction is assumed.
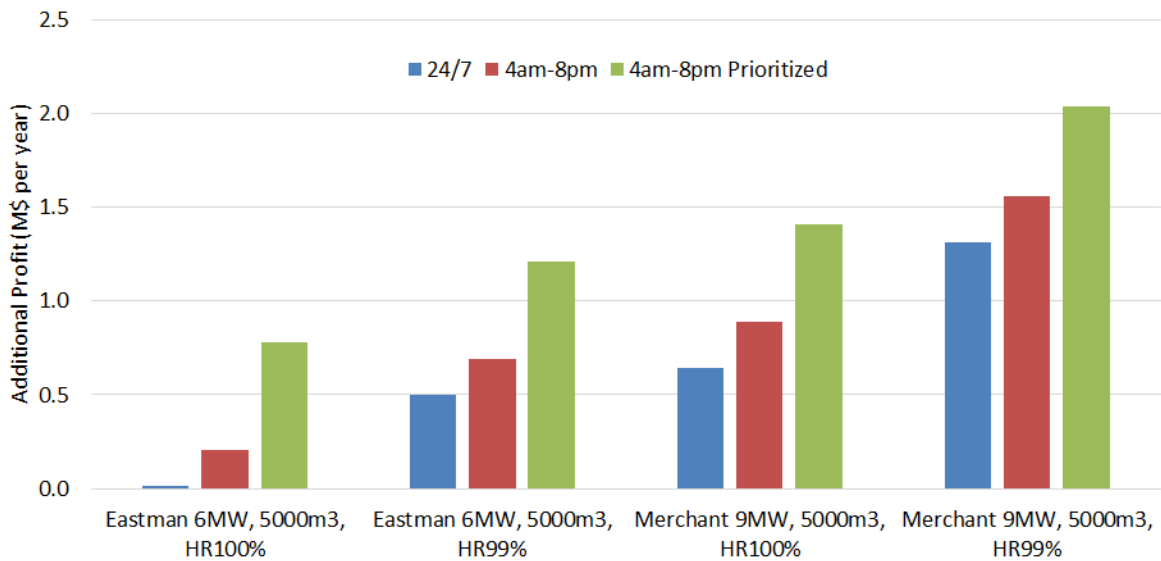
Figure 26. Influence of dispatch logic of different plant cases.

32

A dispatch strategy that sends chilled water to the TIC system whenever available (24/7) is the least cost effective. Constraining this dispatch to the approximate daylight hours (4am-8pm) correlates with power prices and yields higher profit (additional electricity revenue less operating and fuel costs). The best results are found for the most sophisticated dispatch logic, which builds on the 4am-8pm dispatch by looking ahead to hold or dispatch water based on perfect knowledge of future market prices. This "best case" scenario is represented by the "4am-8pm Prioritized" bars.

The team further examined the sensitivity to the capacity of the chiller (MW_t) and tank volume in cubic meters. This was accomplished by comparing the simple payback period while varying the chiller capacity or tank volume. For both plants, a tank larger than 5000 m^3 provides no additional value (Figure 27). Figure 28 shows the payback period results assuming the baseline, i.e., best guess, geothermal conditions (~$4/MMBtu) and costs from the SMU analysis. The small chiller highlights the preference for a smaller CAPEX system due to the marginal economics. The best conditions result in a payback period for the merchant plant of about 16 years.
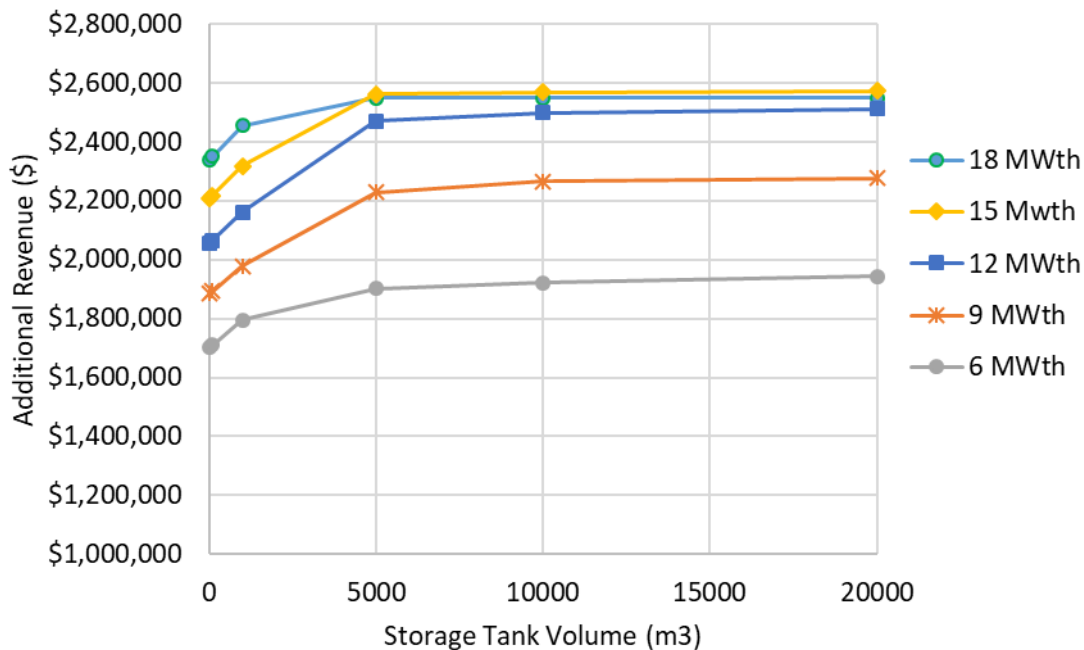
Figure 27. Additional revenue as a function of water tank and chiller capacities. Data shown are for the merchant plant case.
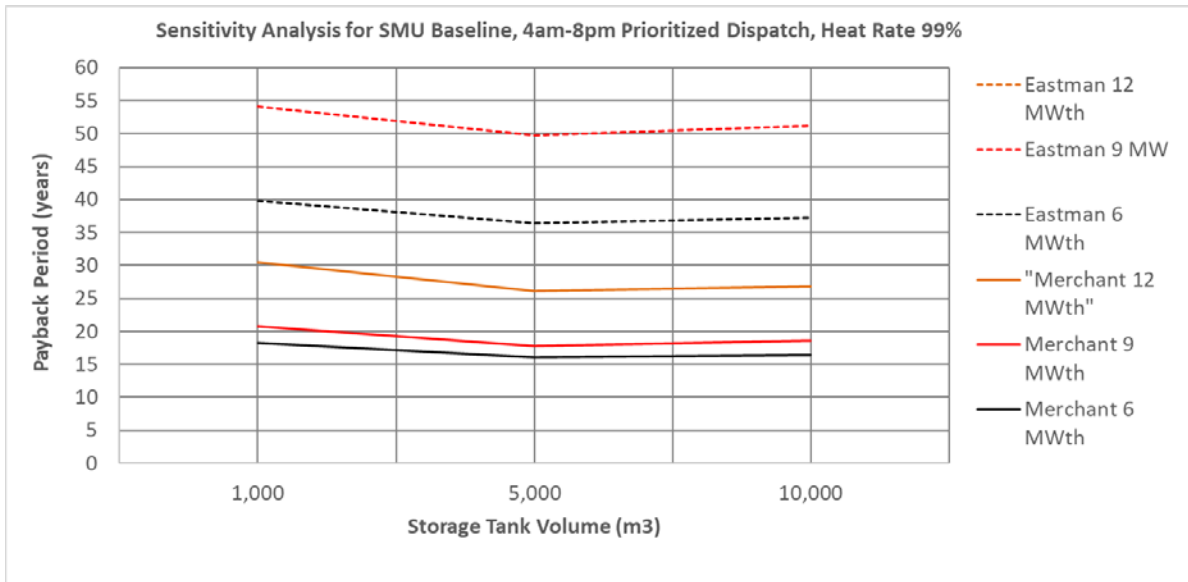
Figure 28. Payback period sensitivity analysis for 4 am-8 pm Prioritized Dispatch logic and 99% relative heat rate at SMU Baseline geothermal conditions ($4/MMBtu).

If one can achieve lower geothermal system costs (for example, $2/MMBtu) the minimum payback period drops from about 16 to 10 years due to the reduced geothermal CAPEX and OPEX (Figure 29).
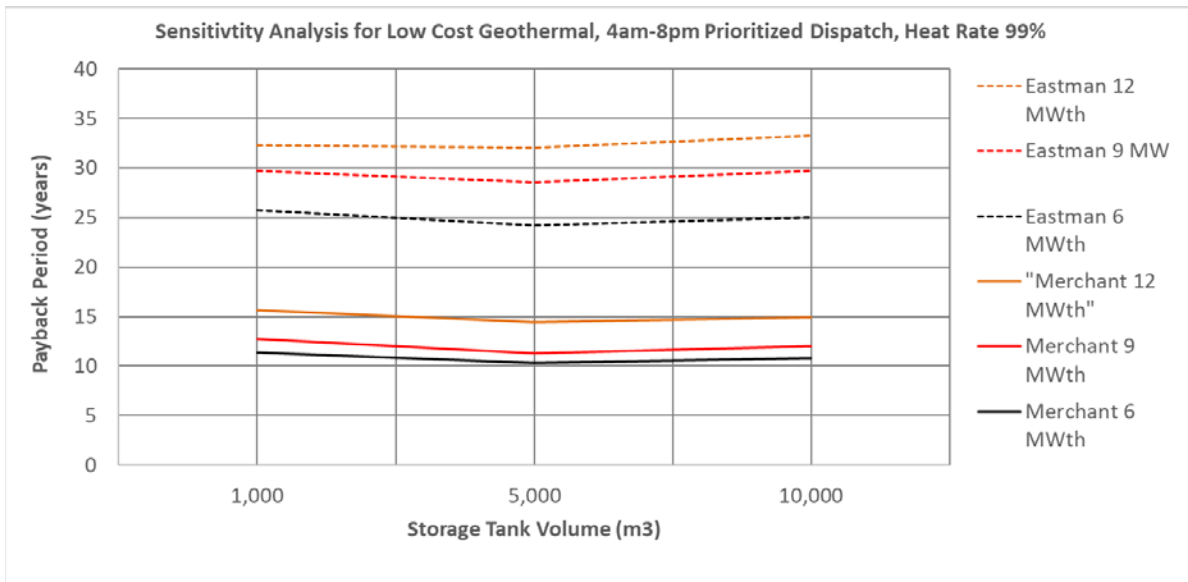
Figure 29. Payback period sensitivity analysis for 4 am-8 pm Prioritized Dispatch logic and 99% relative heat rate at low-cost ($2/MMBtu) geothermal conditions

Lastly, the team estimated net present value (NPV) for the different cases to complete Milestone 3.2. NPV is calculated using the cash flow spreadsheet downloaded from NREL's System Advisor Model (SAM). SAM is packaged with several financial models that can be downloaded as an Excel cash flow spreadsheet. The cash flow spreadsheet from SAM's Generic model,

34

Commercial financing (SAM version 2018-11-11) was used in this study. The major inputs and assumptions for the NPV calculations are given in Table 7.

Table 7. The major inputs and assumptions from SAM financial model

Inputs	Eastman Plant	Merchant Plant
SYSTEM DESIGN		
Chiller Capacity (kW$_t$)	6,000 to 12,000	
Storage Tank (m^3)	1,000 to 10,000	
Dispatch Model	4am-8pm Prioritized	
Relative Heat Rate (vs. non-TIC condition)	0.99	
LOAN PARAMETERS		
Debt fraction (% of total installed cost)	50%	50%
Loan term (years)	18	18
Loan rate (%/year)	7.00	7.00
ANALYSIS PARAMETERS		
Analysis period (years)	30	30
Real discount rate (%/year)	5.00	5.00
TAX AND INSURANCE RATES		
Federal income tax rate (%)	21.00	21.00
State income tax rate (%)	7.00	7.00
Sales tax (% of direct costs)	5.00	5.00

The results are depicted in Table 8, showing that none of the scenarios for an Eastman plant retrofit results in a positive NPV. The combination of higher installed cost due to aspects of a retrofit design and the lower operating capacity factor of the Eastman Chemical Cogen plant factor heavily against the economics. The merchant plant scenario yields positive NPV for most of the cases that assume a more optimistic relative heat rate of 98%. The smaller-capacity chiller systems with 5,000 m^3 water storage tank are favored. The clear benefit of reducing heat rate while deploying TIC is evident. A more detailed operational study than accomplished in this report is necessary to quantify the instantaneous heat rate throughout the year to determine the overall annual benefit that includes temporal prices, weather conditions and plant performance.

Table 8. Comparison of NPV`s for SMU baseline and Low-Cost Geothermal Scenarios at Eastman and Merchant Plants (based on 30-year lifetime)

Plant >		Eastman NPV (M$)				Merchant NPV (M$)			
Geothermal Scenario >		SMU Baseline ($4/MMBtu)		Low-Cost ($2/MMBtu)		SMU Baseline ($4/MMBtu)		Low-Cost ($2/MMBtu)	
Chiller Size (MW$_t$)	Storage Volume (m³)	Heat Rate		Heat Rate		Heat Rate		Heat Rate	
		99%	98%	99%	98%	99%	98%	99%	98%
12	1,000	-$21.54	-$17.37	-$10.63	-$6.46	-$12.08	-$4.92	-$1.17	$5.99
	5,000	-$22.01	-$17.85	-$11.10	-$6.94	-$10.67	-$3.39	$0.24	$7.52
	10,000	-$22.80	-$18.65	-$11.89	-$7.74	-$11.34	-$4.05	-$0.43	$6.86
9	1,000	-$17.02	-$13,27	-$9.50	-$5.29	-$5.84	$1.38	$2.14	$9.36
	5,000	-$17.61	-$13.34	-$9.63	-$5.36	-$3.60	$3.68	$4.38	$11.66
	10,000	-$18.40	-$14.16	-$10.41	-$6.18	-$4.54	$2.82	$3.44	$10.80
6	1,000	-$14.67	-$10.29	-$7.32	-$3.80	-$3.74	$1.18	$3.60	$8.52
	5,000	-$14.47	-$9.79	-$7.13	-$3.30	-$1.75	$4.29	$5.59	$11.63
	10,000	-$15.12	-$10.41	-$7.78	-$3.92	-$2.25	$4.05	$5.09	$11.39

3 Summary and Conclusions

The National Renewable Energy Laboratory (NREL) working with the Southern Methodist University Geothermal Laboratory (SMU), Eastman Chemical, and TAS (Houston, TX) valuated the feasibility of using geothermal heat to improve the performance of a natural-gas power plant in East Texas. The study featured the Eastman Chemical plant in Longview, Texas, which is on the northwestern margin of a geologic region known as the Sabine Uplift. The goal of the project was to determine the technical and economic potential for accessing a geothermal reservoir in the vicinity of the site to provide thermal energy for absorption chillers that would provide chilled water for turbine inlet cooling (TIC) of the plant's combined cycle cogeneration system. Wells within a 20-km radius were included. SMU's review and analysis of available geothermal data indicated a substantial resource in the region, with the Cotton Valley and Travis Peak formations identified as promising targets. The deeper Cotton Valley formation is hotter (approximately 117 to 130°C), yet permeability is only 0.01 to 1.0 mD and porosity less than 12%. The shallower Trinity Group, including the Travis Peak formation, contains much more variability in permeability and porosity and temperatures from approximately 98 to 117°C. The shallower formations are considered despite the lower temperature because of increased ability to produce larger volumes of water and extract enough heat before reinjection. The complete SMU analysis is available in the National Geothermal Data System (NGDS).

A simulation model of the combined cycle power plant was developed in IPSEpro and baselined against operational data from the plant. This model allowed the team to estimate the additional power that could be produced by applying turbine inlet cooling under different operating and ambient conditions. Absorption chiller performance was estimated from vendor sources to determine the production rate of chilled water from the geothermal resource. Geothermal drilling and development costs were estimated using GEOPHIRES 2.0. The expected lower drilling costs in this region led to an estimated cost of geothermal heat of about $4/MMBtu (1.4 cents/kWh$_t$). The estimated cost for the absorption chillers and TIC hardware were obtained from literature sources and project partners.

Hourly data were obtained for weather, natural gas and electricity prices, and plant operating state for 2017, which served as a representative year. NREL estimated the capital cost, operating cost, and additional electricity production and revenue for different combinations of geothermal capacity, chiller capacity, and water storage-tank size. The analysis drove toward smaller geothermal production and chiller systems to reduce CAPEX and allow the storage tank to accumulate the near-continuous chilled water output.

Project economics were explored by calculating a simple payback period and a Net Present Value (NPV), the latter using financial assumptions taken from NREL's System Advisor Model (SAM). The shortest payback period for a plant mimicking operations of the Eastman Chemical plant and using the baseline geothermal assumptions was about 45 years. Lower cost geothermal energy and greater operating capacity factor (i.e., more typical of a merchant power plant) led to payback periods as short as 10 years and positive NPV scenarios. Project life was assumed to be 30 years for the NPV calculations. Such a time frame is more aligned with utility projects than industrial plant investments. The economics were most sensitive to dispatch logic for the TIC system and whether a reduction in heat rate (i.e., increase in thermal efficiency) is obtained during TIC. TIC systems normally result in an improvement in heat rate, but this must be

37

calculated throughout the year, for example on an hourly basis, to quantify the overall net benefit. The current study bounded the likely improvement in heat rate as between 1% and 2%. In addition to heat rate effects, it was essential for TIC system dispatch to track with electric power market prices to maximize revenue.

The study did not lead to economic deployment options for the subject location. Overall economics would be more favorable at locations with wider electric price fluctuations, greater plant capacity factor, and the ability to realize increased efficiency in addition to increased power when applying TIC.

3.1 Project Products

- Josh McTigue and Craig Turchi, "Geothermal energy and thermal storage," Power Plays: Drilling into Geothermal Energy Applications, Southern Methodist University, Dallas, TX, January 10-11, 2018.

- Craig Turchi, J. McTigue, S. Akar, K. Beckers, M. Richards, C. Chickering, J. Batir, H. Schumann, T. Tillman, "Geothermal Deep Direct Use for Turbine Inlet Cooling in East Texas," ASME Energy Sustainability 2020, accepted for presentation.

- Turchi, C., J. McTigue, S. Akar, K. Beckers, T. Tillman, 2018, "Deep Direct-Use for Industrial Application: Producing Chilled Water for Gas-Turbine Inlet Cooling," GRC Transactions, Reno, Nevada, October 15-17, 2018.

- Batir, J., M. Richards, H. Schumann, and S. Fields, "Reservoir Review for Deep Direct Use Project in East Texas," GRC Transactions, Reno, Nevada, October 15-17, 2018.

- GDR/NGDS content ("NGDS" 2019)

  o SMU Fluid Content Model

  o SMU Heat Flow Data

  o SMU Reservoir Parameters

  o SMU Hydraulic Properties Content Model

  o Memo: Phyton Code Calc Q and TaD

  o Memo: Formation Top Mapping

  o Memo: Reservoir Modeling Notes

  o Memo: Hydraulic Properties Model

  o Memo: Heat Flow Extension for East Texas

  o New SMU Well Fluid Production East Texas

  o SMU GRC Paper (Batir, Richards, and Schumann 2018)

  o Part 2 Resource Analysis

References

Ahr, W. M., C. K. Steffensen, and R.C. Faucette. 1984. "Depositional Microfacies and Burial Diagenesis in the Upper Jurassic, Cotton Valley (Haynesville) Limestone, Teague Townsite Field, Texas," 107–17.

Ambrose, W.A., S. P. Dutton, and R.G. Loucks. 2017. "Depositional Systems, Facies Variability, and Their Relationship to Reservoir Quality in the Jurassic Cotton Valley Group, Texas, Louisiana, and Mississippi Onshore Gulf Coast." *GCAGS Explore & Discover Article* 2017 (00238). http://www.gcags.org/exploreanddiscover/2017/00238_ambrose_el_al.pdf.

Ambrose, W.A., T.F. Hentz, F. Bonaffe, R.G. Loucks, L.F. Brown, F.P. Wang, and E.C. Potter. 2009. "Sequence-Stratigraphic Controls on Complex Reservoir Architecture of Highstand Fluvial-Dominated Deltaic and Lowstand Valley-Fill Deposits in the Upper Cretaceous (Cenomanian) Woodbine Group, East Texas Field: Regional and Local Perspectives." *AAPG Bulletin* 93 (2): 37. https://doi.org/DOI:10.1306/09180808053.

Batir, J., M. Richards, and H. Schumann. 2018. "Reservoir Analysis for Deep Direct-Use Feasibility Study in East Texas." *GRC Transactions* 42.

Bearden, Mark D., Casie L. Davidson, Jacob A. Horner, David J. Heldebrant, and Charles J. Freeman. 2016. "Techno-Economic Analysis of Integration of Low-Temperature Geothermal Resources for Coal-Fired Power Plants." PNNL-24879. Pacific Northwest National Lab. (PNNL), Richland, WA (United States). https://doi.org/10.2172/1435895.

Becker, S. P., P. Eichhubl, S. E. Laubach, R. M. Reed, R. H. Lander, and R. J. Bodnar. 2010. "A 48 m.y. History of Fracture Opening, Temperature, and Fluid Pressure: Cretaceous Travis Peak Formation, East Texas Basin." *GSA Bulletin* 122 (7–8): 1081–93. https://doi.org/10.1130/B30067.1.

Beckers, Koenraad F., and Kevin McCabe. 2019. "GEOPHIRES v2.0: Updated Geothermal Techno-Economic Simulation Tool." *Geothermal Energy* 7 (1): 5. https://doi.org/10.1186/s40517-019-0119-6.

Blackwell, D.D., M. Richards, and P. Stepp. 2010. "Texas Geothermal Assessment for the I35 Corridor East, Final Report for Texas State Energy Conservation Office Contract CM709."

Blackwell, D.D., Maria Richards, Zachary Frone, Joe Batir, Andrés Ruzo, Ryan Dingwall, and Mitchell Williams. 2011. "Temperature-At-Depth Maps for the Conterminous US and Geothermal Resource Estimates." In *GRC Transactions*, 35:1545–50. Southern Methodist University Geothermal Laboratory, Dallas, TX (United States). https://www.osti.gov/biblio/1137036-temperature-depth-maps-conterminous-us-geothermal-resource-estimates.

Bruhn, Matthias. 2002. "Hybrid Geothermal–Fossil Electricity Generation from Low Enthalpy Geothermal Resources: Geothermal Feedwater Preheating in Conventional Power Plants." *Energy* 27 (4): 329–46. https://doi.org/10.1016/S0360-5442(01)00088-3.

Bullinger, Charles. 2010. "Lignite Fuel Enhancement." Final Technical Report DE-FC26-04NT41763. Great River Energy.

Camp, Erin. 2016. "GPFA-AB Reservoirs Methodology Memo." https://gdr.openei.org/files/867/Reservoirs_Methodology_Memo.pdf.

Camp, Erin R., Teresa E. Jordan, Matthew J. Hornbach, and Calvin A. Whealton. 2018. "A Probabilistic Application of Oil and Gas Data for Exploration Stage Geothermal

Reservoir Assessment in the Appalachian Basin." *Geothermics* 71 (January): 187–99. https://doi.org/10.1016/j.geothermics.2017.09.001.

Dutton, Shirley P., Stephen E. Laubacht, Robert S. Tye (1, and 2). 1991. "Depositional, Diagenetic, and Structural Controls on Reservoir Properties of Low-Permeability Sandstone, Travis Peak Formation, East Texas" 41. http://archives.datapages.com/data/gcags/data/041/041001/0209.htm.

Dyman, T.S., and S.M. Condon. 2006. "Assessment of Undiscovered Conventional Oil and Gas Resources--Upper Jurassic-Lower Cretaceous Cotton Valley Group, Jurassic Smackover Interior Salt Basins Total Petroleum System, in the East Texas Basin and Louisiana-Mississippi Salt Basins Provinces." USGS Publication No. 69-E-2. USGS. https://pubs.usgs.gov/dds/dds-069/dds-069-e/REPORTS/69_E_CH_2.pdf.

El-Shazly, Alaa A. 2016. "Gas Turbine Performance Enhancement via Utilizing Different Integrated Turbine Inlet Cooling Techniques." *Alexandria Engineering Journal* 55: 1903–14.

EPRI. 2002. "Chillers for Combustion Turbine Inlet Air Cooling." Technical Report 1004352.

———. 2011. "Geothermal/Solar Thermal Hybridization Feasibility." Technical Report 1022118. Palo Alto, CA,.

Ewing, T.E. 1991. "Tectonic Map of Texas." Bureau of Economic Geology." SM0001. Vols. 1:750,000. University of Texas at Austin.

Ewing, Thomas E. 2001. "Review of Late Jurassic Depositional Systems and Potential Hydrocarbon Plays, Northern Gulf of Mexico Basin" 51: 85–96.

Gallardo, Jaquidon, and David D. Blackwell. 1999. "Thermal Structure of the Anadarko Basin." *AAPG Bulletin* 83 (2): 333–61. https://doi.org/10.1306/00AA9A84-1730-11D7-8645000102C1865D.

Gass, T.E. 1982. "Geothermal Heat Pumps." *Geothermal Resources Council Bulletin* 11: 3–8.

Hammes, Ursula, H. Scott Hamlin, and Thomas E. Ewing. 2011. "Geologic Analysis of the Upper Jurassic Haynesville Shale in East Texas and West Louisiana." *AAPG Bulletin* 95 (10): 1643–66. https://doi.org/10.1306/02141110128.

Lowry, Thomas Stephen, John T. Finger, Charles R. Carrigan, Adam Foris, Mack B. Kennedy, Thomas F. Corbet, Christine A. Doughty, Steven Pye, and Eric L. Sonnenthal. 2017. "GeoVision Analysis: Reservoir Maintenance and Development Task Force Report." SAND2017-9977. Sandia National Lab. (SNL-NM), Albuquerque, NM (United States). https://doi.org/10.2172/1394062.

"NGDS." 2019. Search criteria "east texas" + DDU. National Geothermal Data System. 2019. http://geothermaldata.org/.

Pitman, Janet K., and Elisabeth L. Rowan. 2012. "Temperature and Petroleum Generation History of the Wilcox Formation, Louisiana." USGS Numbered Series 2012–1046. Open-File Report. Reston, VA: U.S. Geological Survey. http://pubs.er.usgs.gov/publication/ofr20121046.

Pruess, K., C. Oldenburg, and G. Moridis. 1999. "TOUGH2 USER'S GUIDE, VERSION 2.0." LBNL-43134. University of California, Berkeley, California: Earth Sciences Division, Lawrence Berkeley National Laboratory.

Punwani, D.V. 2008. "Impact of Turbine Inlet Cooling Technologies on Capacity Augmentation and Reduction in Carbon Footprint for Power Production." presented at the Electric Power 2008, Baltimore, MD. http://www.turbineinletcooling.org/News/EP08/Punwani_EP2008.pdf.

Smith, J.D. 2016. "One-Dimensional Heat Conduction Model for Calculating the Surface Heat Flow and Geotherms at Well Locations ", Chapter 3 in J.D. Smith, Analytical and Geostatistical Heat Flow Modeling for Geothermal Resource Reconnaissance Applied in the Appalachian Basin." Ithaca, NY: Cornell University,.

Smith, J.D., and F.G. Horowitz. 2016. "Thermal Model Methods and Well Database Organization in GPFA-AB." Memo 8 in Phase 1 Revised Report of Low Temperature Geothermal Play Fairway Analysis for the Appalachian Basin." https://gdr.openei.org/files/899/GPFA-AB_Final_Report_with_Supporting_Documents.pdf.

Snyder, D.M., K.F. Beckers, and K.R. Young. 2017. "Update on Geothermal Direct-Use Installations in the United States." In *42nd Workshop on Geothermal Reservoir Engineering Stanford University*, 42:7. Stanford, CA: Stanford University. https://pdfs.semanticscholar.org/204c/5bb44fe6fb6eeae70c3af79067e6c77892b7.pdf.

Stutz, George R., Mitchell R. Williams, Zachary Frone, Tim Reber, Maria Richards, David Blackwell, T. E. Jordan, and Jeff Tester. 2012. "A Well by Well Method For Estimating Surface Heat Flow for Regional Geothermal Resource Assessment." In .

Tittman, Jay. 1987. "19. Geophysical Well Logging." In *Methods in Experimental Physics*, edited by Charles G. Sammis and Thomas L. Henyey, 24:441–615. Geophysics. Academic Press. https://doi.org/10.1016/S0076-695X(08)60604-3.

Turchi, Craig, Josh McTigue, Sertac Akar, Koenraad Beckers, and Tom Tillman. 2018. "Deep Direct-Use for Industrial Applications: Producing Chilled Water for Gas-Turbine Inlet Cooling," 16.

Turchi, Craig, Guangdong Zhu, Michael Wagner, Tom Williams, and Daniel Wendt. 2014. "Geothermal/Solar Hybrid Designs: Use of Geothermal Energy for CSP Feedwater Heating." In .

Uddenberg, Matthew Emmanuel. 2012. "An Assessment of Value for Deep Sedimentary Geothermal Resources in Texas." Thesis. https://repositories.lib.utexas.edu/handle/2152/ETD-UT-2012-05-5641.

Vavra, C.L., M.H. Sheihling, and J.D. Klein. 1991. "Reservoir Geology of the Taylor Sandstone in the Oak Hill Field, Rusk County, Texas: Integration of Petrology, Sedimentology, and Log Analysis for Delineation of Reservoir Quality in a Tight Gas Sand." In *The Integration of Geology, Geophysics, Petrophysics and Petroleum Engineering in Reservoir Delineation, Description and Management*. American Association of Petroleum Geologists. https://doi.org/10.1306/SP535C11.

Zafar, S. Daniel, and Bruce L. Cutright. 2014. "Texas' Geothermal Resource Base: A Raster-Integration Method for Estimating in-Place Geothermal-Energy Resources Using ArcGIS." *Geothermics* 50 (April): 148–54. https://doi.org/10.1016/j.geothermics.2013.09.003.

Zhou, Cheng, Elham Doroodchi, and Behdad Moghtaderi. 2014. "Assessment of Geothermal Assisted Coal-Fired Power Generation Using an Australian Case Study." *Energy Conversion and Management* 82 (June): 283–300. https://doi.org/10.1016/j.enconman.2014.03.011.

Appendix 1 - System Schematic for Geothermal Deep Direct Use for TIC

GEOTHERMAL DIRECT USE FOR TURBINE INLET COOLING AT EASTMAN CO-GENERATION PLANT
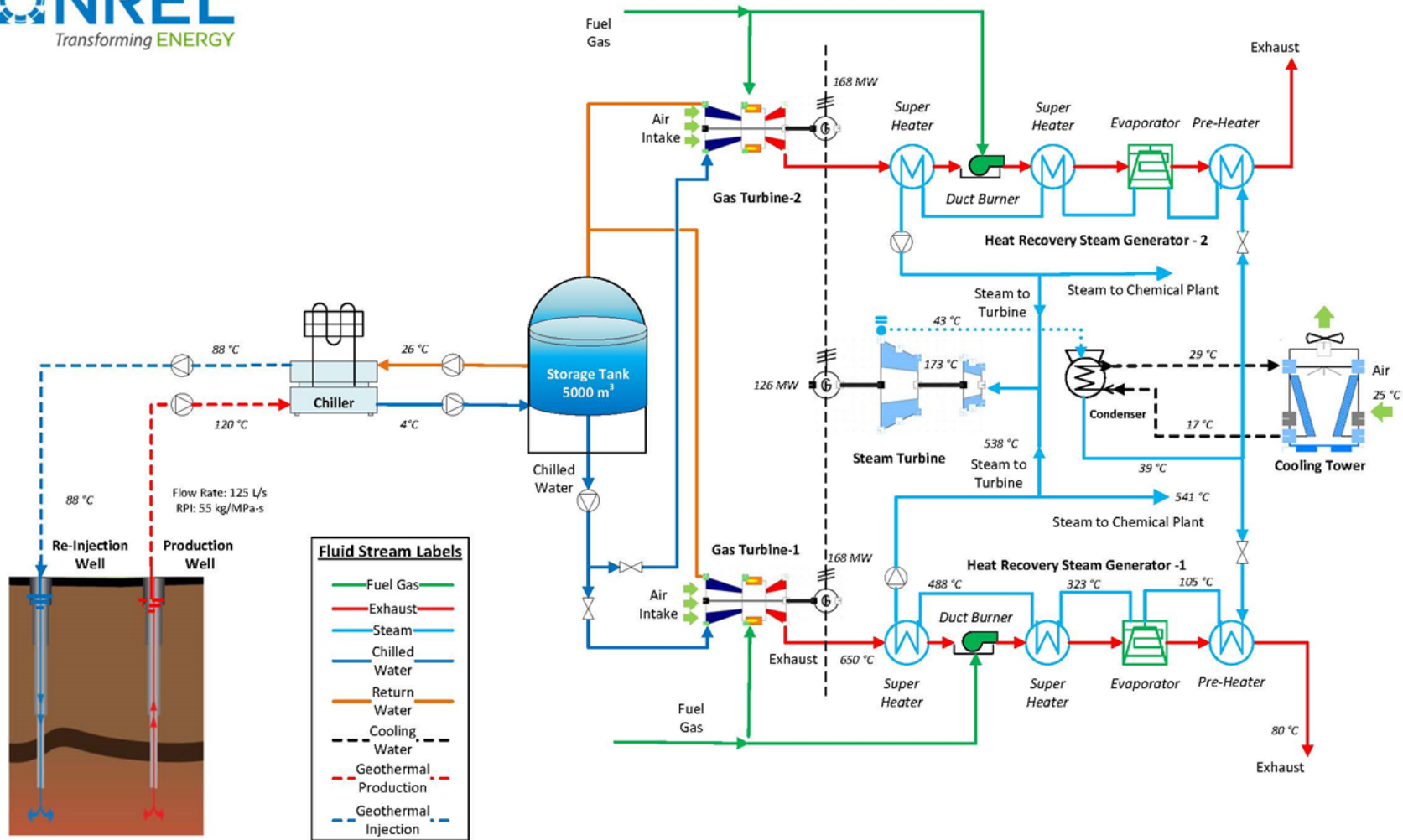
Appendix 2 - Deep Direct-Use Permitting

Author:

Sharon Fields and Maria Richards (mrichard@smu.edu) SMU – Southern Methodist University Geothermal Laboratory, Huffington Department of Earth Sciences, Dallas Texas, 75275

Purpose:

This document describes the permitting process for the Deep Direct-Use project in East Texas as if it were to move forward. In addition to this written document, there is an accompanying spreadsheet listing the Federal, State, and Local permits to obtain and guidelines to follow along with related contacts, documents, or links to them. Together, they cover the main permits required. There are expected to be changes to the permitting process over time and therefore additional permits or changes in the contact persons should be reviewed by future readers of the information.

Key Definitions:

In 1974 the Texas Legislature passed a code within the Natural Resources Act (Title 5: GEOTHERMAL ENERGY AND ASSOCIATED RESOURCES Chapter 141, also cited as the Geothermal Resources Act of 1975), defining geothermal resources as a separate mineral right. The purpose of the code was to provide for the rapid and orderly development of geothermal energy and associated resources located within the State of Texas in the interest of the people of the State of Texas. As defined in Chapter 141, "Geothermal energy and associated resources means: (A) products of geothermal processes, embracing indigenous steam, hot water and hot brines, and geopressured water; (B) steam and other gasses, hot water and hot brines resulting from water, gas, or other fluids artificially introduced into geothermal formations; (C) heat or other associated energy found in geothermal formations; and (D) any by-product derived from them. "By-product" means any other element found in a geothermal formation which is brought to the surface, whether or not it is used in geothermal heat or pressure inducing energy generation."

Scope

To review the permits required, the SMU Geothermal Laboratory began with the OpenEI Rapid Geothermal website, which provides regulatory and permitting information. The materials on the OpenEI Rapid website are generalized for the entire state of Texas with suggestions for agencies to contact for more details. We also worked with Eastman Chemical's permitting office, local government offices, and related agency personnel to determine the necessary permits. This written document is a discussion of the details related to specifically this Eastman Chemical deep direct-use assessment. Therefore, "local" includes the city of Longview, Texas and the 10 km area surrounding the plant site that overlaps with Harrison, Rusk, Panola, and Gregg counties. Taken into consideration are actions necessary if this project moved to implementation, and as an example for similar future deep direct-use projects. We expect permits will be required for at least two wells drilled, one for production and one for reinjection

of fluids used in the direct-use applications, and also for pipe installations to transfer the fluids between the wells and the on-site heat transfer equipment.

Eastman Chemical (EC) manufacturing facility in Longview, Texas includes a natural gas power plant, which generates electricity for EC onsite use, with additional power sold to others via the regional power grid, the Southwest Power Pool (SPP). Thus, there are already existing power purchase agreements between EC and SPP to produce and sell power. It is expected that the existing agreements would be reviewed and updated if more power was made available. To sell into the ERCOT electrical grid, there would need to be new power lines built to connect the plant to this grid with an additional cost for the project. As of now, we are not including that effort as part of our permitting process review.

The following explanation of the permits follow the OpenEI Rapid Geothermal outline structure for ease of future users of this document. It provides an example of a project most likely on privately owned land, such as EC or an individual landowner. We also include the review of permits for the state and federal lands nearby.

Location

The regional area within a 10 km radius of the Eastman Chemical (EC) power plant was reviewed for surface land ownership. Figure 1 is a picture of the central portion of the main EC site, which depicts the industrial density of their property where their production processes and power plant are located. The power plant is located the northwest corner of the property near Interstate Highway 20 (I-20). EC owns approximately 6,000 acres with both surface and mineral rights for a portion of it. There are existing oil and gas wells on this property. The goal of the project is to use land fully owned (surface and mineral) as the best-case scenario, both to limit the impact on the neighbors and to reduce expenses. Bordering land to the EC property in this SE area is primarily rural land, owned by individuals as homes or ranches.

In reviewing the permitting process for this assessment, we took into consideration that a surface pipe carrying fluids could be installed either on-site or as far out as 10 km. Ten kilometers was used as the maximum possible distance to pipe hot fluids to a project site. Within this 10 km area there are a few main items to contend with for permitting. These include I-20 to the north adjacent to their property, the City of Longview with high building density to the Northeast, the Sabine River to the South and its related floodplain and wetlands. Further south of the river is a regional airport that the project would not cross based on distance and difficulty obtaining permits. If off-site property must be used, the most realistic well and surface piping location based on permitting is to the east or southeast between the interstate and the river.

Federal and State Regulatory Agencies

Any geothermal deep direct-use project in Texas must comply with the Federal and State environmental protection laws. There are different agencies overseeing the permits/regulations for them. If the project is funded by a government agency such as the Department of Energy, a National Environmental Policy Act (NEPA) review is required to assess the environmental and related social and economic impacts of a project. The Environmental Protection Agency (EPA) regional office in Dallas, Texas would oversee the primary environmental concerns within a NEPA study. Congress has designated the EPA as the federal regulatory body responsible for writing the standards for clean air, clean water, waste disposal, and underground injection

control. In addition to the EPA, the Fish and Wildlife Service (for East Texas, regional office is in Albuquerque, New Mexico) oversees the Endangered Species and Migratory Bird Acts.

For the State of Texas, the Texas Commission on Environmental Quality (TCEQ) oversees the site-specific related permits for air emissions, water supply, surface waste disposal, non-hazardous injection of fluids, and the Facility Operating Area (FOA) designation. For example, EC already has a FOA designation associated with their chemical plant facility.

The drilling of wells and the production of the deep non-potable water from them is permitted by the Texas Railroad Commission (RRC). The reinjection of that water is also permitted through the RRC as determined by the TCEQ Underground Injection Control Program to fall within the Class V Injection Well category. This Class V permit covers the reinjection of the produced fluids after they go through the surface processes to make the chilled water for cooling. The main difference between the production fluid and injection fluid is the reduced heat content of the fluid. Due to the high amounts of dissolved minerals expected in the water chemistry, these produced fluids are required to be reinjected into formations below the freshwater aquifers.

Land Access

In Texas the land-use planning process is governed at the municipal level. Under Chapter 213 of the Texas Local Government Code (TLCG), land use planning in Texas is delegated to municipalities. The EC property is located Southeast of the City of Longview, the county seat for Gregg County. However, the main plant is located within Harrison County. Rusk and Panola Counties are also part of the (10 km radius) potential project area. Longview is the closest county seat to the EC power plant, therefore in discussing permitting applications with them, we were able to work through their office. The planning office in Longview works with the county seats in Marshall (Harrison County), in Henderson (Rusk County), and Carthage (Panola County) helping to coordinate the permitting process. If the project moves forward with drilling the wells, then permits are obtained through each of the counties as their location deems necessary.

The placement of the wells determines where a water pipeline is located. The permitting for the pipeline starts with the Railroad Commission (RRC) and local city and county government offices. Once the pipeline is built, the Railroad Commission district office in Kilgore becomes responsible for the pipeline safety oversight.

The permitting process for locating a pipeline from a production well to the EC power plant for use of the fluids, and then piped to an injection well for disposal takes into consideration the land ownership and ease of access to cross it. For this assessment, we took into consideration two planning concerns for permitting as they include public land: 1) crossing Interstate Highway 20, and 2) crossing the Sabine River and floodplain. If the wells for this project are drilled north of Interstate Highway 20, then the United States Department of Transportation and the Texas Department of Transportation (TxDOT) district offices (Fort Worth for this area) would be involved and permits related to the right of way (ROW) are required for the pipeline to cross it. TxDOT district offices protect the state's right of way (ROW) through permits and coordination of the safe and efficient operation of Texas highways. It is expected that multiple ROW permits will be necessary for the pipeline to cross the county and local roads depending on where the production and injection wells are located. Any land crossed by a pipeline will need to have

45

owner approval, leasing agreements, and appropriate permits. Regarding crossing the Sabine River and floodplain, see the discussion below.

The City of Longview also has permits and will assist people with the permitting process. There are requirements locally for land use planning, pipeline leases, and oil and gas operations (which geothermal wells are expected to fall under).

Surface Water

Texas surface water rights and resulting permits are through the Texas Commission on Environmental Quality (TCEQ). This project would use wells below the surface aquifers and not inject water into surface streams or fresh aquifers.

If wells are drilled to the south of the EC property, a pipeline would need to cross the Sabine River and/or floodplain, resulting in the need for a permit from the U.S. Army Corps of Engineers. The Sabine River crosses into Louisiana and therefore is an interstate river. Depending on who owns the riverbanks where a pipeline crosses, additional permits will be necessary: from the Texas General Land Office if state owned land, from local county offices if county/city owned, or via leasing permits if private property.

Well Drilling and/or Conversion

The production and injection wells could be existing wells converted for use in this project or new wells drilled to meet the fluid quantity requirements. Either situation will involve the RRC and its oil and gas, and geothermal permits. There are permits for drilling a well, recompletion of well (change in well type with work-over), etc. The RRC Drilling Permits (W-1) User Guide is recommended reading for a full list of permits and understanding of when they are necessary.

Well Maintenance and Oversite

Once the deep direct-use geothermal production wells are flowing fluids, a Production Test Completions Report (GT-1) will be required by the RRC. There will also be an Injection Well Pressure Test Report (H-5). There are additional recurring reports that must be reported to the RRC for monitoring both the well integrity and fluid production and injection. The Kilgore District 6 office assists in getting them initiated and reviews the submissions.

On-Site Power Plant

The primary physical changes that would take place at the surface of the EC power plant include the building of a large storage tank and additional pipes between the tank and the inlet cooling application. These changes will require building permits and construction permits. Working with the local, City of Longview Planning Office and City Engineer will provide the full list of permits and approvals required. As additional power is available to sell with improved efficiency, there may need to be a new or revised purchase power agreement between EC and Southwest Power Pool.

Contacts for Permit and Regulations in Longview, Texas

Land Use Planning Longview Texas Planning Zones 903-237-1030 Permit/Application 903-237-1074 Public Works Dept. 903-237-1240	Planning & Zoning Department City of Longview's Engineering Dept. P.O. Box 1952 Longview, TX 75606 Andrew Fields 903-237-1362
TXDOT-Atlanta District www.txdot.gov/inside- txdot/district/atlanta.html Harrison County 701 E Main Street Atlanta, Texas 75551 Fax 903-799-1229	Director of Maintenance Jason Dupree, P.E. Office 903-799-1248 Mobile 512-95-1846
TXDOT-Tyler District www.txdot.gov Rusk County/Gregg County 2709 W. Front St. Tyler, TX 75702 800-558-9368 Fax 903-510-9158	TxDOT Utility Permitting Office Karen.Gardner@txdot.gov RRC Railroad Commission of Texas www.rrc.state.tx.us Mailing Address PO Box 12967 Austin, TX 78711-2967 Physical Address 1701 N. Congress Austin, TX 78701 Main telephone line: 877-228-5740 publicassist@rrc.texas.gov
Tyler District Maintenance 903-510-9203	Environmental Permitting Department Geothermal Projects 512-463-3840
TCEQ Texas Commission on Environmental Quality www.tceq.texas.gov ac@tceq.texas.gov Engineering Dept. 512-239-6696 Brian Dickey- Plan Review Team @Water Supply Division Brian.dickey@tceq.texas.gov 512-239-0963	GLO Texas General Land Office State Lands Mailing Address PO Box 12873 Austin, TX 78711-2873 512-463-5001 Physical Address Energy Resources 1700 N. Congress Avenue Austin, TX 78701-1495
Colby Eaves colby.eaves@glo.texas.gov 512-463-5326	

47

(ACEC) Areas of Critical Environmental Concern: "ACEC designations highlight areas where special management attention is needed to protect important historical, cultural, and scenic values, or fish and wildlife or other natural resources. ACECs can also be designated to protect human life and safety from natural hazards. ACECs can only be designated during the land-use planning process." https://www.blm.gov/programs/planning-and-nepa/planning-101/special-planning-designations/acec

(BLM) Bureau of Land Management: "The BLM manages more than 245 million acres of public land located primarily in 12 Western states, including Alaska. The BLM also administers 700 million acres of sub-surface mineral estate throughout the nation. The agency's mission is to sustain the health, diversity, and productivity of America's public lands for the use and enjoyment of present and future generations." www.blm.gov

(BOR) Bureau of Reclamation: Established in 1902, the mission of the BOR is to manage, develop, and protect water and related resources in an environmentally and economically sound manner in the interest of the American public. It is best known for the construction of dams, power plants and canals in 17 western states, including the western panhandle of Texas. BOR operates 53 power plants and is the second largest producer of hydroelectric power. They are also the largest wholesaler of water in the nation. At this time, there are no projects within the northeast part of Texas near the study area. https://www.usbr.gov/

(CNN) Certificate of Convenience and Necessity: a certificate granting its holder "exclusive right to provide retail water and/or sewer utility services to an identified geographic area. Chapter 13 of the Texas Water Code requires a CCN holder to provide continuous and adequate service to the area within the boundary of its CCN. Municipalities and districts normally are not required to have a CCN; however, some municipalities and districts do have a CCN. A district or municipality may not provide retail water or sewer services within an area for which another utility holds a CCN unless the district or municipality has a CCN for the area." Certificated Service Areas fall into one of three types: Bounded, Facilities +200 feet, and Facilitates Only. See Public Utility of Texas (PUCT) for additional information. http://www.puc.texas.gov/. https://www.puc.texas.gov/industry/water/utilities/gis.aspx

(Corp or The Corps) U.S. Army Corp of Engineers: The organization responsible for environmental engineering for the nation. In addition to support of all branches of the U.S. military, The Corps owns and operates over 600 dams, 12,000 miles of navigable channels, and maintains

(CWA) Clean Water Act: As described at https://www.epa.gov/laws-regulations/summary-clean-water-act, the Clean Water Act 33 U.S.C. §1251 et seq. (1972) "establishes the basic structure for regulating discharges of pollutants into the waters of the United States and regulating quality standards for surface waters… Under the CWA, EPA has implemented pollution control programs such as setting wastewater standards for industry. EPA has also developed national water quality criteria recommendations for pollutants in surface waters." It "is the primary federal law governing water pollution." In Texas, the Texas Commission on Environmental Quality, or TCEQ, is responsible for monitoring.

(DOD) Department of Defense

(DOE) Department of Energy

(DOI) Department of Interior

(EIS) Environmental Impact Statement   "provides the framework for the USFS to address pending geothermal lease applications"

(EIS) Environmental Impact Statements: A document prepared either by or for the Environmental Protection Agency which identifies and analyzes, in detail, environmental impacts of a proposed action, as required by the National Environmental Policy Act (NEPA). There are very limited examples of EIS for geothermal projects in Texas at the time of this report. The Department of Energy provided an EIS for a DOE sponsored project in western Texas in 2011 that could serve as a document outline, to be adapted for a project in east Texas. https://www.energy.gov/sites/prod/files/EIS-0444-FEIS-Summary-2011.pdf, upon approval from EPA Region 6.

(EPA) Environmental Protection Agency: Federal agency missioned with protection of human health and the environment. This broad mandate includes, in part, ensuring Americans have access to clean air, land and water, that contaminated lands are cleaned, that toxic substances are reviewed, and that environmental stewardship is considered in development of U.S. policy. EPA develops and enforces regulations, such as implementation of the Clean Water Act, the Clean Air Act, and others. East Texas is governed by Region 6. https://www.epa.gov/aboutepa/our-mission-and-what-we-do

(ERCOT) Electricity Reliability Council of Texas

(FERC) Federal Energy Regulatory Commission

(FLPMA) Federal Land Policy and Management Act of 1976 : Law "designed to provide guidance for future management actions and the development of subsequent, more detailed and limited scope plans for resources and of Land uses." https://www.blm.gov/or/regulations/files/FLPMA.pdf

(FWS) Fish and Wildlife Service

(GDP) Geothermal Drilling Permit

(GLO) Texas General Land Office

(LT) Land Trade

(LUP) Land Use Plan: It dictates what can and cannot be done on the managed unit of land.

(MFPs) Management Framework Plans

(NEPA) National Environmental Policy Act: Signed into law in 1970, 42 U.S.C. §4321 et seq. (1969) "requires federal agencies to assess the environmental effects of their proposed actions prior to making decisions." It encompasses decisions regarding permit applications, federal land management, and construction public owned facilities, such as highways. Depending upon the decision at hand, multiple federal agencies may be involved. The Office of Federal Activities will coordinate the input of multiple agencies. https://www.epa.gov/nepa and https://www.epa.gov/laws-regulations/summary-national-environmental-policy-act

(NPDES) National Pollutant Discharge Elimination System: the program for discharge control as defined by the Clean Water Act. https://www.epa.gov/npdes/about-npdes. It regulates point sources that discharge pollutants into waters of the United States. Monitoring is principally a state effort, with only four states (ID, NM, MA and NH) and designated Indian Country handled by the EPA. NPDES permits are required for any facility to discharge directly into a U.S. body of water.

(NPSP) Nonpoint Source Pollution

(NRDC) National Resources Defense Council

(OFA) Office of Federal Activities: Responsible for coordination of the EPA's review of all federal Environmental Impact Statements (EIS) prepared by other agencies under NEPA, as well as EPA's compliance with NEPA.

(POU) Plan of Utilization: Completed as part of projects to produce geothermal resources and convert to marketable electricity.

(PSF) Permanent School Fund

(PUCT) Public Utility Commission of Texas

(RA) Relinquishment Act: Mineral rights held by State of Texas and managed under the GLO, who must approve all terms including bonus consideration, royalty rates, and rental amounts, and any additional provisions for any RA lands.

(RCRA) Resource Conservation and Recovery Act: Authorizes the EPA to manage hazardous waste.

(READ-Database) Renewable Energy and Defense Geospatial Database: Department of Defense developed mapping and analytical tool providing geographic information systems data. The objective is to allow renewable energy developers to locate appropriate sites for renewable projects (e.g. utility-scale wind, solar, and geothermal energy) that "are unlikely to interfere with military activities and training and have the fewest environmental conflicts." Available through the NRDC (National Resources Defense Council) website by submitting a request. https://www.nrdc.org/resources/proactive-planning-tool-renewable-energy-development

(REC) Renewable Energy Credit Program: RECS are issued when one megawatt-hour (MWh) of electricity is generated and delivered to the electricity grid from a renewable energy resource.

(RMP) Resource Management Plan: Applicable Land Use Plan for public lands filled out under the Bureau of Land Management.

(ROD) Record of Decision: A resource management plan submitted to the Federal agency overseeing the land.

(ROW) Right-of-Way

(RRC) Railroad Commission of Texas: "The Railroad Commission of Texas was established in 1891 under a constitutional and legislative mandate to prevent discrimination in railroad charges and establish reasonable tariffs. It is the oldest regulatory agency in the state and one of the oldest of its kind in the nation." Today, its responsibility for regulating all oil and gas drilling and production is a major function. They also regulate drilling and operation of geothermal wells, transportation of geothermal fluids, and other relevant permits and reporting. www.rrc.state.tx.us

(SPP) Southwest Power Pool: Grid operators for the region to the east and north of Longview, Texas. SPP is a member of NERC North American Electric.

(TCEQ) Texas Commission on Environmental Quality

(TLCG) Texas Local Government Code

(TMDLs) Total Maximum Daily Loads

(TPWD) Texas Parks & Wildlife Department

(TSSWCB) Texas State Soil and Water Conservation Board

(UIC) Underground Injection Control Permit

(USFS) United States Forest Service

(UST) Underground Storage Tank